(5)

Report DT-8203-01

AD A117245

Dynamics Technology, Inc.

DESIGN AND LABORATORY TESTING OF A PROTOTYPE LINEAR TEMPERATURE SENSOR

C. Michael Dube and Christian M. Nielsen

Dynamics Technology, Inc.
22939 Hawthorne Blvd., Suite 200
Torrance, California 90505

1 July 1982

Final Report for Period 1 January 1982 - 30 June 1982

UNLIMITED DISTRIBUTION

Prepared for

OFFICE OF NAVAL RESEARCH
Department of the Navy, Code 614A
800 N. Quincy
Arlington, Virginia 22217

NAVAL OCEAN RESEARCH AND DEVELOPMENT ACTIVITY
Code N68462
Mr. K. M. Ferer, Code 500
NSTL Station, Mississippi 39529

This report has undergone an extensive internal review before release, both for technical and non-technical content, by the Division Manager and an independent internal review committee.

Division Manager:

Duane T. Howe

Internal Review:

Robert L. Gram

UNCLASSIFIED

SECURITY CLASSIFICATION OF THIS PAGE (When Data Entered)

REPORT DOCUMENTATION PAGE		READ INSTRUCTIONS BEFORE COMPLETING FORM
1. REPORT NUMBER DT-8203-01	2. GOVT ACCESSION NO.	3. RECIPIENT'S CATALOG NUMBER
4. TITLE (and Subtitle) DESIGN AND LABORATORY TESTING OF A PROTOTYPE LINEAR TEMPERATURE SENSOR		5. TYPE OF REPORT & PERIOD COVERED FINAL REPORT 1 January 82 - 30 June 1982
		6. PERFORMING ORG. REPORT NUMBER DT-8203-01
7. AUTHOR(s) C. Michael Dube Christian M. Nielsen		8. CONTRACT OR GRANT NUMBER(s) N00014-82-C-0122
9. PERFORMING ORGANIZATION NAME AND ADDRESS Dynamics Technology, Inc. 22939 Hawthorne Blvd., Suite 200 Torrance, California 90505		10. PROGRAM ELEMENT, PROJECT, TASK AREA & WORK UNIT NUMBERS
11. CONTROLLING OFFICE NAME AND ADDRESS Office of Naval Research Dept. of the Navy Code 614A 800 N. Quincy St., Arlington, VA 22217		12. REPORT DATE June 1982 13. NUMBER OF PAGES 63
14. MONITORING AGENCY NAME & ADDRESS (if different from Controlling Office) Naval Ocean Research and Development Activity Code N68462 NSTL Station, MS 39529 ATTN: Mr. K. M. Ferer, Code 500		15. SECURITY CLASS. (of this report) UNCLASSIFIED 15a. DECLASSIFICATION/DOWNGRADING SCHEDULE

16. DISTRIBUTION STATEMENT (of this Report)

Approved For Public Release; Distribution Unlimited.

17. DISTRIBUTION STATEMENT (of the abstract entered in Block 20, if different from Report)

18. SUPPLEMENTARY NOTES

19. KEY WORDS (Continue on reverse side if necessary and identify by block number)

Oceanographic instruments
Internal waves

20. ABSTRACT (Continue on reverse side if necessary and identify by block number)

This report discusses the basic theory, design, and laboratory testing of a prototype linear temperature sensor (or "line sensor"), which is an instrument for measuring internal waves in the ocean. The operating principle of the line sensor consists of measuring the average resistance change of a vertically suspended wire (or coil of wire) induced by the passage of an internal

DD FORM 1 JAN 73 1473 EDITION OF 1 NOV 65 IS OBSOLETE

UNCLASSIFIED

wave in a thermocline. The advantage of the line sensor over conventional internal wave measurement techniques is that it is insensitive to thermal finestructure which contaminates point sensor measurements, and its output is approximately linearly proportional to the internal wave displacement.

An approximately one-half scale prototype line sensor module was tested in the laboratory. The line sensor signal was linearly related to the actual fluid displacement to within 10%. Furthermore, the absolute output was well predicted (within 25%) from the theoretical model and the sensor material properties alone. Comparisons of the line sensor and a point sensor in a wavefield with superimposed turbulence (finestructure) revealed negligible distortion in the line sensor signal, while the point sensor signal was swamped by "turbulent noise." The effects of internal wave strain were also found to be negligible.

The prototype line sensor is of rugged design and was intended for direct scaling to an ocean-going version. Included in this report is a detailed preliminary design for an ocean-going line sensor composed of several line sensor modules suspended vertically, including data acquisition and processing circuitry for internal wave modal analysis. Dynamics Technology recommends further development of a full-scale prototype line sensor based on the highly successful results of this study.

SUMMARY

This report discusses the basic theory, design, and laboratory testing of a prototype linear temperature sensor (or "line sensor"), which is an instrument for measuring internal waves in the ocean. The operating principle of the line sensor consists of measuring the average resistance change of a vertically suspended wire (or coil of wire) induced by the passage of an internal wave in a thermocline. The advantage of the line sensor over conventional internal wave measurement techniques is that it is insensitive to thermal finestructure which contaminates point sensor measurements, and its output is approximately linearly proportional to the internal wave displacement.

An approximately one-half scale prototype line sensor module was tested in the laboratory. The line sensor signal was linearly related to the actual fluid displacement to within 10%. Furthermore, the absolute output was well predicted (within 25%) from the theoretical model and the sensor material properties alone. Comparisons of the line sensor and a point sensor in a wavefield with superimposed turbulence (finestructure) revealed negligible distortion in the line sensor signal, while the point sensor signal was swamped by "turbulent noise." The effects of internal wave strain were also found to be negligible.

The prototype line sensor is of rugged design and was intended for direct scaling to an ocean-going version. Included in this report is a detailed preliminary design for an ocean-going line sensor composed of several line sensor modules suspended vertically, including data acquisition and processing circuitry for internal wave modal analysis. Dynamics Technology recommends further development of a full-scale prototype line sensor based on the highly successful results of this study.

PREFACE

This report documents work carried out during the period 1 January through 30 June 1982 under ONR Contract N00014-82-C-0122. We gratefully acknowledge the sponsorship of the Office of Naval Research and the valuable technical discussions with Mr. Ken Ferer of NORDA.

The authors wish to acknowledge several individuals who made significant contributions to the success of this project: Mr. John Jaacks, Ms. Dotty Jost, Dr. Dennis McLaughlin, Mr. Joe Moross, and Mr. Dennis Plocher.

Special recognition is given to Dr. Robert L. Gran for his continued support and initial theoretical work which formed the basis for this project.

TABLE OF CONTENTS

1. INTRODUCTION

The measurement and characterization of internal gravity waves in the ocean's thermoclines is of obvious importance to the U.S. Navy. Not only are such waves naturally ubiquitous, but also the passage of a vessel within or near a thermocline generates internal waves which may be discernible from the background waves. The characteristics of deep water and fairly long wavelength internal waves are now fairly well-known from conventional oceanographic measurements.[1] This is not the case for internal waves in the seasonal thermocline, however, especially for the shorter wavelengths ($\lesssim$ 100m) which are typically generated by localized sources.

Most existing internal wave measurement systems are inadequate for measuring these relatively short waves. This inadequacy stems from two sources; either the sensor response is so contaminated by what is known as oceanic finestructure that a correlation with other similar response measurements is virtually meaningless, or such enormous amounts of data need to be gathered at several measurement stations that the processing and correlation of the recorded data would be extremely inefficient. An example of sensors which exhibit the former inadequacy could be an array of thermistors, even if held stationary in the ocean, whereas examples of the latter type of inadequacy could be several temperature-versus-depth "yo-yo" profilers. This is not to say that such sensors do not have their own particular advantages in measuring certain phenomena, only that the identification of internal wave propagational

[1] Konvayev, K.V. and Sabinin, K.D. (1972) "New Data on Internal Waves in the Ocean Obtained With Distributed Temperature Sensors," Doklady Akad. Nauk SSSR, 209 (Geophysics).

characteristics (and, possibly, the detection of particular internal waves within a seemingly random background) might be unnecessarily complicated with these sensors.

Recently, the use of a new type of internal wave sensor has been reported in Russian technology papers[1,2] in which vertically extensive temperature-sensitive sensors of from one to one hundred meters in length have been employed. The basic output of such a linear temperature sensor, or "line sensor," is an electrical resistance change which is directly proportional to the temperature change of the surrounding water over the depth range of the sensor caused by the vertical displacement of a passing internal wave. Because of the temperature averaging characteristic of such a sensor, it is much less sensitive to variations in the detailed temperature-depth profile (the so-called microstructure) and, because of its nearly linear response, it is a relatively easier task to correlate this signal with other such signals in order to extract the propagational characteristics of passing internal waves.

Two practical considerations regarding a line sensor are that the thermal inertia of the line sensor must be small enough so that the electrical resistance accurately tracks the water's temperature (by using thin wire and avoiding contact with massive structural supports) and that other resistance changes (e.g., changes due to wire stretching caused by fluid dynamic drag variations) are sufficiently small. Addressing these practical issues and actually designing and testing a prototype line sensor formed the basis of the

---

[2] Brekhovskikih, L.M., Konjaev, K.V., Sabinin, K.D. and Serikov, A.N. (1975) "Short-Period Internal Waves in the Sea," J. Geo. Res., 80, No. 6, February.

work reported herein. Based on the success of the laboratory prototype, a second phase of development should be to actually deploy line sensors in an ocean thermocline along with conventional internal wave instrumentation in order to obtain data for a direct comparison to assess its future utility.

Section 2 of this report presents a review of the fundamental operating principles of the line sensor and a derivation of the internal wave displacement inferred from the line sensor output. Section 3 discusses the prototype sensor design and Section 4 describes the laboratory experimental facility. Results of the experiments are presented in Section 5, and a suggested ocean-going line sensor design is outlined in Section 6. Section 7 contains the summary and conclusions of this six month investigation.

2. REVIEW OF LINE SENSOR OPERATING PRINCIPLES

In this section, the response to internal gravity wave displacements by an ideal line sensor of finite length immersed in an arbitrarily (but stably) stratified volume of water is described (following the original analysis of Gran and Kubota[3]). By "ideal," it is meant to imply the following considerations:

a. Infinitesimal heat capacity of the line sensor material and supporting structure

b. Inviscid, non-diffusive flow of the surrounding water about the line sensor and its supporting structure.

2.1 Response Equation

Consider the situation illustrated in Figure 1 which represents a body of stably stratified water ($d\rho/dz < 0$, where ρ is the density of the fluid and z is the vertical position measured upward). Shown also are several isotherms which were originally at a depth ζ but which, because of the passage of an internal wave, have become displaced vertically an amount δ depending on when and where one looks during the passage of the wave. The vertically oriented line sensor is also shown on this figure by the solid heavy line. The length of the line sensor is L and its mid-point is at a depth z_c.

---

[3] Gran, R.L. and Kobuta, T. (1977) "The Response of a Distributed Linear Temperature Sensor to Internal Waves in a Microstructure-Laden Ocean," Dynamics Technology Report DT-7601-21.

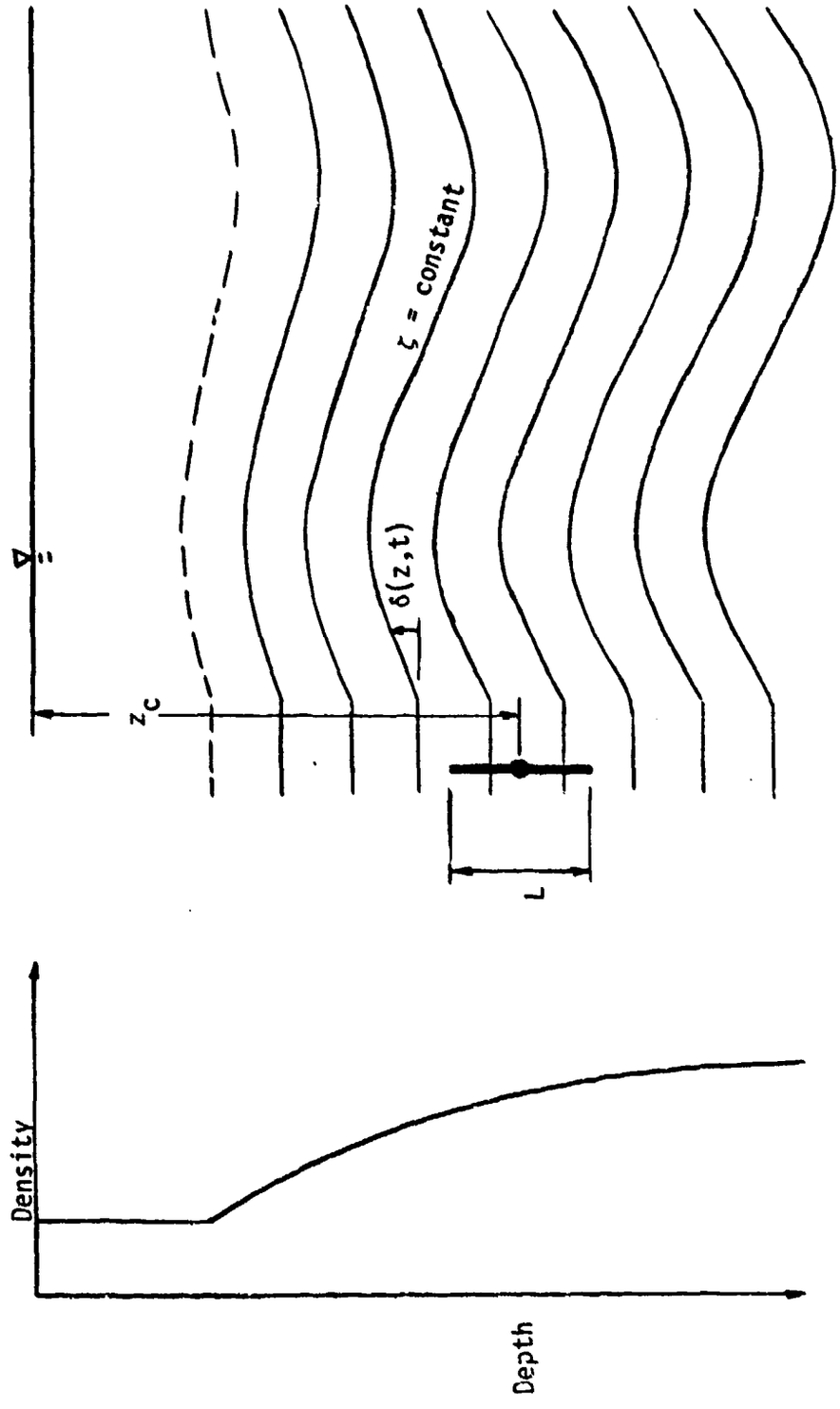

Figure 1. Vertical Fluid Density Profile and Schematic Representation of Isotherm Displacements Caused by an Internal Wave

The line sensor is presumed to be constructed of a material, such as thin wire whose electrical resistance changes with temperature, which is "strung" upon a supporting structural framework. The electrical resistance of this wire at a reference temperature T_o (say, 0°C) is r_o ohms per meter of wire length. If the wire temperature, T_w, is different from T_o, then the electrical resistance per meter of length is determined from the linear relation;

$$r = r_o \left[1 + \alpha(T_w - T_o)\right] \tag{2.1}$$

where α is the temperature-resistance coefficient which has a value for most common conducting metals on the order of 0.1% per degree centigrade. The neglect of higher-order terms is predicated on the small temperature changes perceivable by an *in situ* line sensor.

Because of the infinitesimal heat capacity, it is implicit that the wire's temperature is always equal to the water temperature at the same depth and that the water temperature profile is described by $T(z,t) = T(\zeta)$ where $\zeta = \zeta(z,t)$; and the quantity ζ identifies an isotherm. Thus, the total resistance of the line sensor is

$$R(t) = R_o + \alpha r_o \int_{z_c - L/2}^{z_c + L/2} \Delta T(\zeta)\, dz \tag{2.2}$$

where $$\Delta T \equiv T(\zeta) - T_o \ .$$

Further, since $R_o = r_o L$, Equation 2.2 may be written as:

$$R(t) = R_o \left\{ 1 + \frac{\alpha}{L} \int_{z_c - L/2}^{z_c + L/2} \Delta T(\zeta(z,t)) dz \right\} . \qquad (2.3)$$

The change in the total line sensor resistance from some initial time t = 0 is more relevant to the measurement of internal waves (since the second term in the above equation is usually small compared to unity) and this is

$$\Delta R(t) \equiv R(t) - R(o) = \alpha R_o \left\{ \frac{1}{L} \int_{z_c - L/2}^{z_c + L/2} [T(\zeta(z,t)) - T(\zeta(z,o))] dz \right\} . \qquad (2.4)$$

Note that the expression within the braces represents the change in the average water temperature over the depth of the line sensor and is independent of the properties of the temperature-sensitive wire. These wire properties just define the constant of proportionality. In order to maximize the output signal of the line sensor, this product should then be maximized by not only the selection of the wire material but also its size (diameter) and total length.

Returning to the derived expression for the line sensor response to internal wave-induced water temperatare changes (which is exact provided the assumptions made are valid) one would like to know under what conditions the sensor output $\Delta R(t)$ is linearly proportional to the internal wave displacement in the vicinity of the line sensor (say, $\zeta(z_c,t) - \zeta(z_c,0)$). Two such cases have been found for which such a linear relation holds. The first of these is the case where the ambient water vertical temperature gradient is strictly

constant and where the internal wave displacement field is strain free (that is $\zeta(z,t) = z + \delta(t)$ so that $\partial z/\partial \zeta = 1$; in other words, the vertical separation between any two isotherms remains constant). Then

$$\Delta R(t) = \alpha R_o \left(\frac{dT}{dz}\right)_o \delta(t) \doteq \alpha R_o \left(\frac{\overline{\Delta T}}{L}\right) \delta(t) \ . \tag{2.5}$$

where $\overline{\Delta T}$ is the temperature change over the length of the line sensor.

The second interesting case is where only two isothermal layers adjoin one another at an interface whose displacement, $\delta(t)$, is never beyond the ends of the line sensor. Then, again

$$\Delta R(t) = \alpha R_o \left(\frac{\overline{\Delta T}}{L}\right) \delta(t) \tag{2.6}$$

where $\overline{\Delta T}$ is the temperature difference between the two isothermal layers (which, again, is equal to the temperature difference over the length of the line sensor).

Of course, if the prevailing ambient water and internal wave characteristics were not exactly described by either of these two situations, then the sensor output signal would not be linearly related to the internal wave displacement. In fact, to encounter such conditions (such as a strictly constant temperature gradient or a single temperature step) in an oceanic environment would be extremely unlikely, so that even with an ideal line sensor, some nonlinear distortion between the actual water displacement and the line sensor output will probably be present. The question then is; can the characteristics of the line sensor (say, its length, for example) be selected so that this nonlinear distortion is either negligible or, at the least, minimal so as to not invalidate the ultimate use of the line sensor?

In order to illustrate an extreme example of this nonlinear distortion refer to the bottom of Figure 2 where the response of a very short line sensor (a point sensor) immersed in a measured oceanic internal wave field is depicted. This should be compared to the measured displacement history which is shown in the middle of Figure 2. (Both of these isotherm displacement histories were calculated by Nesnyba, *et al.* (1972),[4] from internal wave measurements, such as those shown in the upper portion of Figure 2, obtained in deep Arctic waters from a floating ice station). Regarding the internal wave record shown at the top of Figure 2, note the prominent sheets-and-layers structure of the ambient temperature distribution. Referring once again to

[4] Neshyba, S., Denner, W.W. and Neal, V.T. (1972) "Spectra of Internal Waves: In-Situ Measurements in a Multiple-Layered Structure," J. Phys. Ocean., 2, p. 91, January.

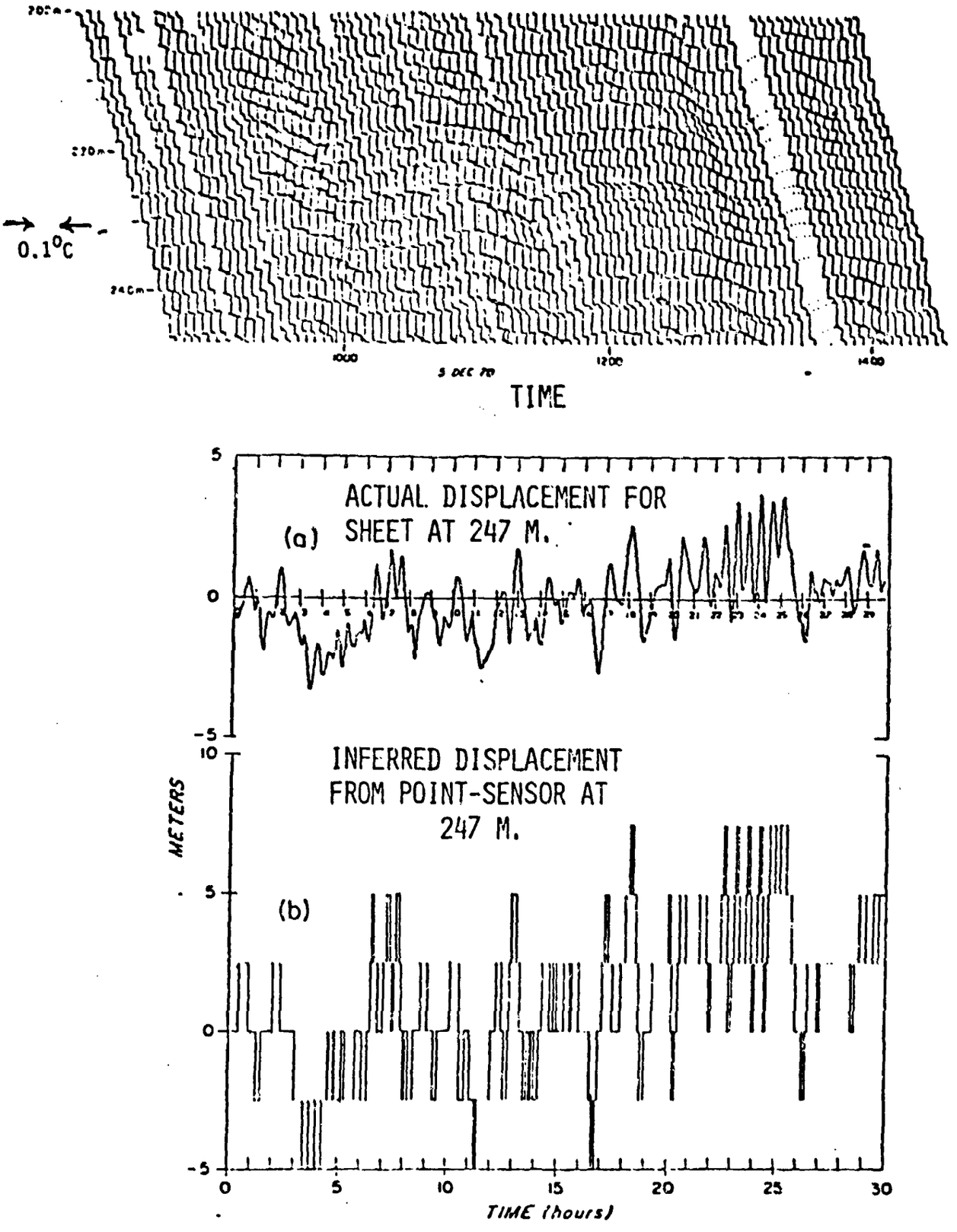

Figure 2. Measurements of Oceanic Internal Waves and Comparison of Actual Versus Inferred Displacements (from Neshyba *et al.*)

the two sheet displacement records, note that although there is some there is some correspondence between these two, the point sensor output is highly and irreversibly distorted from the actual displacement history and it is unlikely that two or more such distorted records could confidently be used to determine the propagational characteristics of such waves.

2.2 Inversion of Line Sensor Response

In the previous section, an exact expression for an ideal line sensor response to isotherm displacements was derived. Only in certain special cases was this response linearly related to the true isotherm displacement. An approximate inversion of the general expression for the line sensor resistance change (Equation 2.4), which yields an estimate of the internal wave displacement δ from the measured resistance change was derived by Gran and Kubota.[3] The assumptions in the inversion relation are:

(1) The fluid vertical strain is small over the length of the line sensor (i.e., the internal wave vertical wavelength $\Lambda_v >> L$, the line sensor length).

(2) The line sensor spans several finestructure "layers," so that the temperature difference between the top and bottom of the line sensor $\overline{\Delta T} >> \tau$, the temperature jump across an isolated layer.

(3) The line sensor mean temperature is nearly zero, if measured relative to the line sensor centerline temperature, so displacements can be referenced to the centerline displacement $\delta_c(t)$.

These assumptions can all be made valid by proper choice of the line sensor length. The resulting expression for the line resistance change is

$$\Delta R(t) \doteq \alpha R_o \left(\frac{\overline{\Delta T}}{L}\right) \delta_c(t) \left[1 + O\left(\frac{L^2}{\Lambda_v^2}, \frac{\delta_c}{L} \cdot \frac{L}{\Lambda_v}, \frac{\tau}{\overline{\Delta T}}\right)\right] \tag{2.7}$$

This approximate relation is to first-order identical to the two previously mentioned exact relations. The terms included in the O( ) symbol imply that some error is involved in using the most simple relation between $\Delta R(t)$ and $\delta_c(t)$ but its accuracy should be adequate if the line sensor length is much shorter than Λ_v but longer than either the maximum isotherm displacement or the isothermal layer thickness (so that $\tau << \overline{\Delta T}$). It is noted that these second-order corrections could be evaluated if the vertical structure of the internal wave(s) and ambient temperature profile were both known. This is usually not the case, especially if one is measuring random oceanic internal waves which typically contain energy from many sources. Because of its simplicity, however, and the fact that equation (2.7) agrees with the two exact relations discussed previously, (equations (2.5) and (2.6)), equation (2.7) will be used as an estimate of the true fluid displacement in the vicinity of the line sensor. This estimate will be denoted as $\hat{\delta}(t)$ where

$$\hat{\delta}(t) = L(\alpha\overline{\Delta T})^{-1} \frac{\Delta R(t)}{R_o} \tag{2.8}$$

In order to get a figure-of-merit for a line sensor which is a measure of the degree-of-distortion, a computational algorithm has been devised. From the computed values of $\hat{\delta}_i$ (the inferred fluid displacement) a least-squares-fit to the equation $\hat{\delta} = B\delta$ (where δ is the actual displacement) may be found. Then, the degree-of-distortion, DD, is defined as

$$(DD)^2 = \frac{\sum (\hat{\delta}_i - B\delta)^2}{\sum (B\delta)^2} \tag{2.9}$$

Thus, DD^2 is the normalized mean-square deviation between the inferred fluid displacement and the best linear fit to the actual displacement. If, for example, DD were 0.1, then from a number of (normally distributed) displacement inferences $\hat{\delta}_i$ more than two-thirds of them should be within 10% of the actual fluid displacement at the center of the line sensor. This figure-of-merit is applied to the experimental data described in Section 5.

3. PROTOTYPE LINE SENSOR DESIGN

A prototype line sensor was designed and constructed for testing in an existing 2.4 m long x 0.6 m wide x 1 m deep tank in the Dynamics Technology Laboratory. The depth of the tank constrained the line sensor length to about 50 cm (allowing for significant vertical motion and clearance from the bottom and surface).

Several constructive concepts were considered during the design phase. When deployed in the ocean, the line sensor will be a rather long instrument (~ 10-100 m), therefore, some method for compact storage must be incorporated in the design. The notions of wrapping a fine wire around a flexible cable or stringing wire inside an open mesh tube, for example, were considered. Bringing the temperature sensitive wire in close contact with a structural support will greatly reduce its sensitivity because of the large thermal inertia associated with a massive object compared to a fine wire. (Researchers at the Johns Hopkins University, Applied Physics Laboratory, constructed a prototype line sensor by wrapping wire around a plastic pipe and achieved poor results.) Placing wires inside a mesh tube, while difficult to fabricate, might produce a workable design, however, the difficulties involved in isolation of failures, repair, and potential sensor wire straining (which produces anomalous resistance changes) lead us to reject this approach. In the end, a modular design was chosen in which the sensing element is enclosed in a rigid frame as described below. This design permits free flow of water past the sensing wire, eliminates any significant strain on the wires by the support structure

(fluid strains are negligible, see Reference 3), allows flexibility in the overall sensor length, facilitates easy failure isolation and repair, and lends itself to compact storage (i.e., the module can be folded together, see Section 6).

It was desired to construct a laboratory sensor that simulated as closely as possible a single module of an ocean-going version of the line sensor. The intent is to "string together" several similar modules to form a field prototype for ocean testing in Phase II of the development effort. The basic design of the laboratory prototype line sensor probe is shown in Figure 3.1. The sensing element consists of 10 m of 10 mil nickel wire with a 3 mil Teflon coating (1 mil = 25.4 μm). The wire is strung back-and-forth between two Nylon rods 50 cm apart, supported in a stainless steel rectangular tubing frame. A wire mesh screen may be mounted on each side of the frame to prevent physical damage to the sensor (e.g., falling debris, handling, etc.).

For an ocean-going line sensor, this module would be extended to approximately 1 m length/module, and several such modules could be strung together. However, even one 1 meter line sensor module could form a functional internal wave sensor; additional modules improve microstructure rejection and yield more extensive internal wave information. Details of a suggested ocean-going line sensor design are discussed in Section 6.

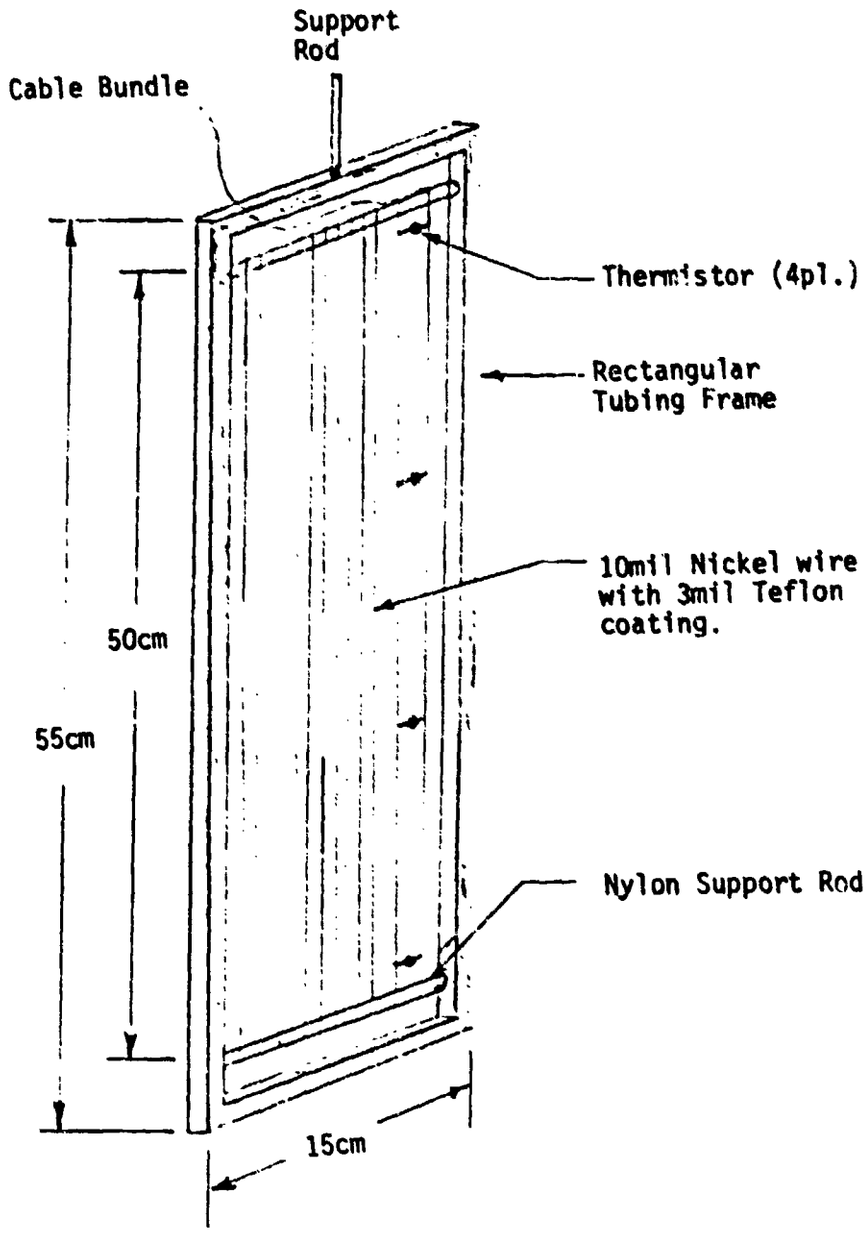

Figure 3.1. Laboratory Prototype Line Sensor.

The determination of internal wave-induced fluid displacement requires measurement of the small temperature-induced changes in the line sensor's electrical resistance. Recalling equation (2.11), the fractional change in the line sensor's resistance is approximately,

$$\frac{\Delta R}{R_o} = \alpha\left(\frac{\overline{\Delta T}}{L}\right) \delta_c \qquad (3.1)$$

where α is the temperature coefficient of resistance (measured as $0.0055°C^{-1}$), $\overline{\Delta T}/L$ is the ambient water's temperature gradient at the line sensor location (typically ~ 0.05°C/m in the ocean), and δ_c is the internal wave amplitude. In order to measure wave amplitudes as small as 10 cm in the ocean, therefore, the measuring system should resolve $\Delta R/R_o$ to within 30 parts in a million. This serves to establish a design electronic noise level for the line sensor circuit.

Originally, it was planned to employ the line sensor as one leg of a DISA 56C01 commercial hot-film anemometer bridge run in the (constant current) temperature sensor mode. This unit produces a wideband amplified signal with a large (5 volt) D.C. offset. Despite various filters applied to the output of this anemometer, an unacceptable noise level still remained which was traced to a local AM radio station. The line sensor acted as an antenna and the wideband DISA amplifier (Gain = 10^4) passed the modulated signal.

To solve this problem, a small inductor was inserted in series with the line sensor to attenuate the RF signal. Also, a bridge more tailored to the line sensor's resistance and a filtered amplifier section were designed and built which produced greatly reduced noise levels. The final line sensor bridge circuit is shown in Figure 3.2.

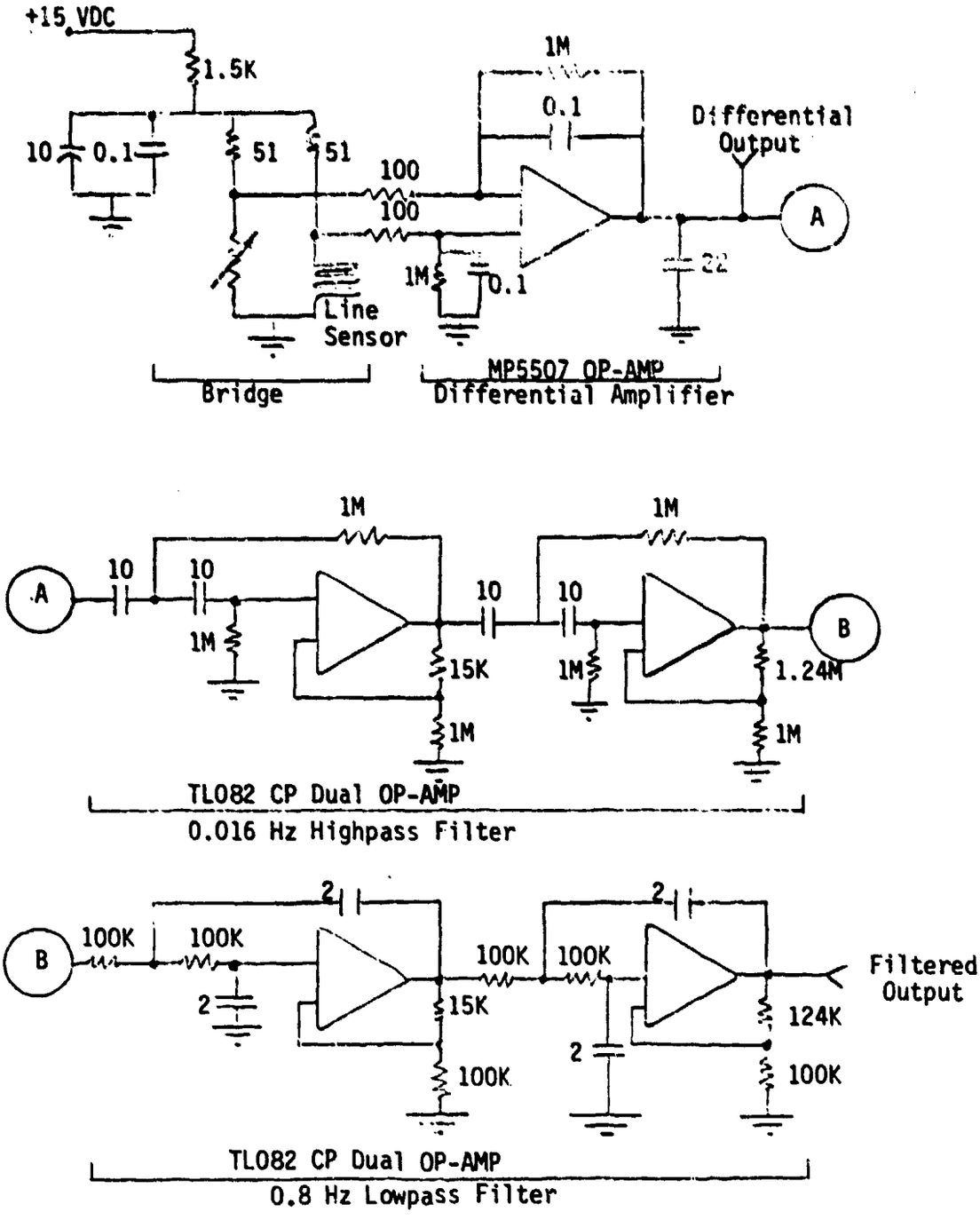

Figure 3.2 Electrical Schematic of Line Sensor Circuit

The resistance of the line sensor (R_0 = 33 ohms) is balanced by a variable resistor in the opposite leg of the D.C. bridge. The bridge voltage is amplified by 10^4 and is then passed through a four pole Butterworth bandpass filter (0.016 - 0.8 Hz). The signal from the differential amplifier may also be monitored directly. The filter introduces a frequency dependent time delay and uniform gain which must be accounted for when comparing filtered and reference waveforms. The time delay would not, however, affect the spectral content of the filter output. It was found that the output from the differential amplifier actually met the noise specification ($\Delta R/R_0 < 3 \times 10^{-5}$) without additional filtering and this output was used as the primary line sensor signal in some of the later laboratory experiments, since it has the advantage of no phase delay.

Using the measured bridge sensitivity of 2.37 volt/ohm, and a filter gain of 4.0 the noise equivalent $\Delta R/R_0$ and the noise equivalent "fluid displacement" rms levels (for an oceanic system) of the differential amplifier and the filter's output with the laboratory line sensor were,

	rms $\Delta R/R_0$	rms Equivalent Fluid Displacement
Differential Amp.	1.3×10^{-5}	4.6 cm
Filtered Output	$\sim 3 \times 10^{-6}$	$\sim$ 1.1 cm

In principle, the laboratory prototype line sensor could be deployed in the ocean to measure natural internal waves. Of course, other considerations such as contamination of such measurements by natural ocean finestructure dictate that a longer line sensor be used in the ocean than was developed for the laboratory (see Section 6).

4. TEST FACILITY DESCRIPTION

The objective of the experiments was to verify the linear response of a prototype line sensor, to compare it to the theoretical response, and also to determine other characteristics of the line sensor such as its response time, sensitivity and durability. To accomplish this, the general scheme utilized was to generate a relative motion between the line sensor and thermally stratified water either by moving the line sensor through the stratified water or by generating internal waves in the tank while holding the line sensor fixed. The test facility arrangement is shown in a sketch in Figure 4.1 and in a photograph, Figure 4.2. A computer based data acquisition system (DAS) was used to record several relevant quantities and subsequently to reduce the data. This section describes the thermal stratification method, the line sensor and wave generator drive mechanism, the DAS and data reduction method, and the line sensor test procedure.

4.1 Stratification Method

Most of the experiments were carried out with either a near linear temperature profile or a "step" temperature profile (see Figure 4.3). By also adding varying amounts of salt to the water, the thermocline was found to be exceptionally stable, remaining fairly constant for periods up to four hours. The general procedure followed was to first fill the lower half of the tank with salt water (specific gravity ≈ 1.025) and the upper half with fresh water. A 9 KW heater was then used to heat the fresh water for a pre-determined time. By carefully stirring only the fresh water, a fairly sharp step

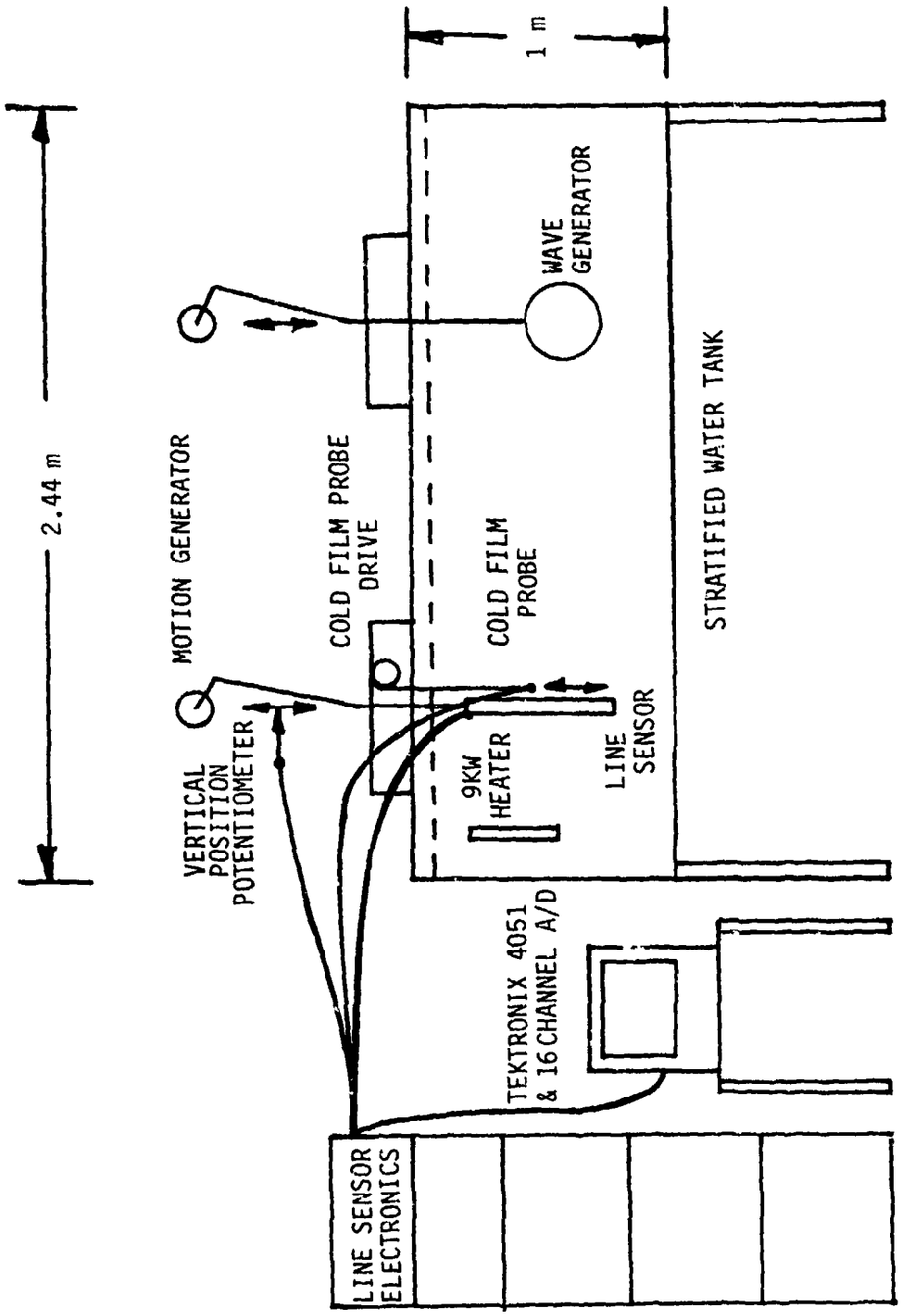

Figure 4.1 Test Facility Layout

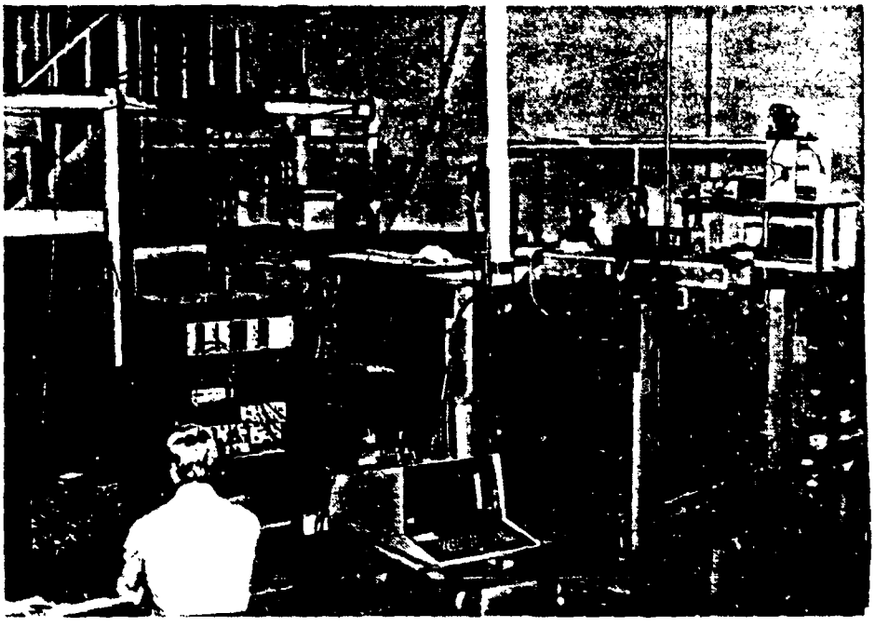

Figure 4.2 Photograph of Test Facility

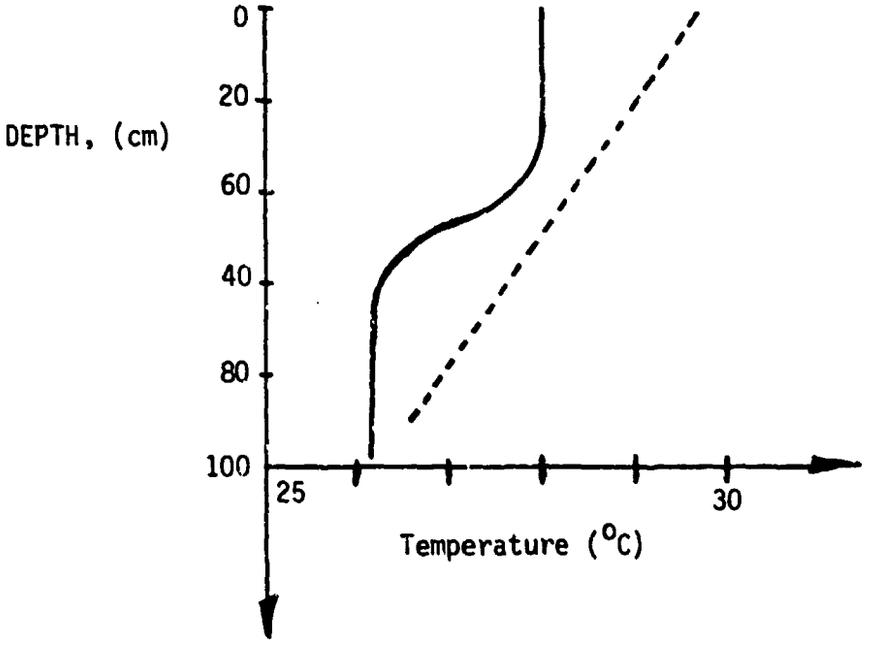

Figure 4.3 Typical Linear (Dashed) and "Step" Temperature Profiles Generated

temperature profile was obtained. By vigorously stirring the entire tank and then allowing it to settle, an approximately linear temperature profile was obtained.

4.2 Line Sensor and Wave Generator Drive Mechanism

A simple motion generator was designed and constructed to generate a vertical displacement approximately sinusoidal in time. This device was used to drive the line sensor in still water during experiments to measure actual displacement of the line sensor and to determine the linearity of the line sensor's response by comparing to the inferred displacement. Alternatively, the device was connected to a large cylinder (~ 20 cm diameter) and used to generate internal waves.

The motion generator was driven by a 1/20 HP universal gear motor with a speed range of 1 to 4 rpm. A direct current power supply was used as the controller. The vertical displacement of the motion generator is adjustable from 3 to 13 cm, and a calibrated linear potentiometer was connected to the vertical displacement rod to automatically record the depth history.

4.3 Data Acquisition System and Data Reduction

The Data Acquisition System (DAS) is based on a TransEra analog-to-digital (A/D) converter interfaced to a Tektronix 4051 computer. Typical quantities measured simultaneously include the line sensor resistance change directly from the differential bridge and through a bandpass filter, the vertical position of the motion generator with the linear potentiometer, and the bridge outputs of various point sensors such as thermistors and the "cold

film" probe. Additionally, the computer was used to record the temperature versus depth profile before and after the experiments measured with a DISA 55R11 film probe mounted on a mechanical drive and connected to a DISA 56C01 CTA unit and 56C10 bridge operated in the constant current (temperature sensing) mode.

Software was developed for the Tektronix computer for data reduction and plot generation. Values are calculated for the inferred line sensor displacement ($\hat{\delta}$) and two error parameters, the instantaneous normalized error (ε), and the average linear distortion (DD) defined in equation (2.9). The inferred displacement is given by:

$$\hat{\delta} = - \frac{V_f L}{S_b G_f \alpha R_o \overline{\Delta T}} , \tag{4.1}$$

where: V_f = the filtered line sensor output voltage,

L = the line sensor length,

S_b = the bridge sensitivity (V/Ω),

G_f = the filter gain,

α = the thermal coefficient of resistance of the line sensor material ($°C^{-1}$),

R_o = the line sensor resistance at 0°C,

$\overline{\Delta T}$ = the average temperature difference between the top and bottom of the line sensor.

The two error parameters are defined as:

$$\varepsilon = \frac{\hat{\delta} - \delta}{|\delta|_{max}} , \text{ and} \tag{4.2}$$

$$DD = \left[\frac{\sum (\hat{\delta} - B\delta)^2}{\sum (B\delta)^2} \right]^{1/2} , \tag{4.3}$$

where: $\hat{\delta}$ = the inferred displacement (equation 4.1),

δ = the actual displacement

B = the proportionality constant between δ and $\hat{\delta}$ as determined by a least squares fit to the equation

$$\hat{\delta} = B\delta \ .$$

The error parameter ε is the normalized instantaneous difference between the actual and inferred displacements, and the distortion parameter, DD, represents the average nonlinear distortion of the inferred displacement.

4.4 Procedure

The general procedure for all tests was as follows. The salinity stratified tank was heated, stirred, and allowed to "settle" to obtain the desired temperature profile (i.e., residual fluid motions from internal waves had decayed to imperceptible levels). All electronic instruments were switched on, allowed to warm up, and subsequently calibrated. The mean temperature profile was measured and the output ranges of the line sensor and vertical position potentiometer were checked to verify the electronics. The drive motor on the line sensor or wave generator was then switched on and adjusted to the desired speed.

With the system calibrated and functioning smoothly, the data acquisition was begun. While data was being recorded on the computer, critical quantities such as the line sensor's voltage, vertical position and, occasionally, a point sensor were also monitored in real time on a digital oscilliscope. At the test's conclusion, the temperature profile was again measured for any change and all data was stored for subsequent analysis.

5. EXPERIMENTAL RESULTS

All line sensor tests reported in this section were performed in the DynaTech free-surface, stratified water tank facility (Figure 4.1) following the general procedure described in Section 4. Specific tests were performed to isolate and best illustrate individual properties and, combined, the tests provided a data base for the stability and ruggedness of the line sensor probe. Specific properties of the prototype line sensor which were tested were:

1) the linearity of the response (inferred vs. actual displacement),
2) the response time,
3) the effect of thermal finestructure, and
4) the effect of internal wave strain.

Additionally, experiments were performed for specific mechanical design considerations, the effect of protective cover screens and of sensor wire insulation loss. In the remainder of this section, a brief description of the test and results are organized into the following subsections:

5.1 Linearity - Comparison With Theory

The linearity tests were performed by driving the line sensor probe through the thermally stratified water with the sinusoidal motion generator. The temperature profiles were measured before and after the experiment using the cold film probe. The line sensor's output voltage from the bridge (V_b) and filter (V_f) were measured along with the vertical position potentiometer output voltage (V_p).

The actual displacement (δ) was computed using equation (5.1.1) and the inferred displacement ($\hat{\delta}$) was computed using equation (4.1) repeated below for convenience. The average temperature difference across the line sensor was estimated from the measured temperature profile and mean line sensor probe position.

$$\delta = K_p V_p \tag{5.1.1}$$

$$\hat{\delta} = - \frac{V_f L}{S_b G_f \alpha R_o \overline{\Delta T}} \tag{4.1}$$

In equation (5.1.1), K_p is the calibration factor for the potentiometer and was measured to within ~5%. The accuracy of the inferred displacement is determined from the root-mean-square of the estimated error in each of the terms on the right-hand side of equation (4.1).

$$\frac{d\hat{\delta}}{\hat{\delta}} = \left[\left(\frac{dV_f}{V_f} \right)^2 + \left(\frac{dL}{L} \right)^2 + \left(\frac{dS_b}{S_b} \right)^2 + \left(\frac{dG_f}{G_f} \right)^2 + \left(\frac{d\alpha}{\alpha} \right)^2 + \left(\frac{dR_o}{R_o} \right)^2 + \left(\frac{d\overline{\Delta T}}{\overline{\Delta T}} \right)^2 \right]^{1/2} \tag{5.1.2}$$

A resolution estimate indicated the following limits: (for variable definitions, see equation (4.1), Section 4.)

$$\frac{dV_f}{V_f} \approx \pm .005$$

$$\frac{dL}{L} \approx \pm .005$$

$$\frac{dS_b}{S_b} \approx \pm .05$$

$$\frac{dG_f}{G_f} \approx \pm .05 \qquad (5.1.3)$$

$$\frac{d\alpha}{\alpha} \approx \pm .01$$

$$\frac{dR_o}{R_o} \approx \pm .01$$

$$\frac{d\overline{\Delta T}}{\overline{\Delta T}} \approx \pm .05$$

Substituting the above estimates gives the expected error in the inferred displacement:

$$\left|\frac{d\hat{\delta}}{\hat{\delta}}\right| < 0.09 .$$

When combined with the 5% error in the actual displacement, this indicates a maximum expected error of 14% between the actual and inferred displacements, i.e.

$$\left|\frac{\hat{\delta}-\delta}{\delta}\right| < 0.14 . \qquad (5.1.4)$$

The results of three linearity tests are shown in Figures 5.1.1, 5.1.2 and 5.1.3. The first two are for "step" profiles (5°C and 1°C steps, respectively), and the third case is a linear profile. The temperature profiles before and after each test (displaced by + 1°C) are shown in the lower right hand corner along with the line sensor's extent. Note also that the third case (Figure 5.1.3) differs from the first two in that the line sensor signal utilized is the bridge voltage (V_b) instead of the filtered voltage (V_f). The calculation of the inferred displacement remains the same, except that V_b is input to equation (4.1) instead of V_f and the filter gain (G_f) is 1.0 .

The run conditions, wave period, peak-to-peak displacement amplitude, filter lead time, and filter gain, are listed in the upper left corner along with the linear proportionality constant (B) and linear distortion (DD). The actual displacement (δ) is plotted against the inferred displacement ($\hat{\delta}$) in the upper right hand corner. The left-hand side of these figures consists of four curves: (from top to bottom) the actual displacement (δ), the inferred displacement ($\hat{\delta}$), the two overlayed, and the instantaneous error (ε).

The linear proportionality constant (B) is determined by a least squares fit to:

$$\hat{\delta} = B\delta \ . \qquad (5.1.5)$$

The instantaneous error ε is computed from equation (4.2):

$$\varepsilon = \frac{\hat{\delta}-\delta}{|\delta|_{max}} \ . \qquad (4.2)$$

B and ε can be approximately bounded by using (5.1.4), i.e.,

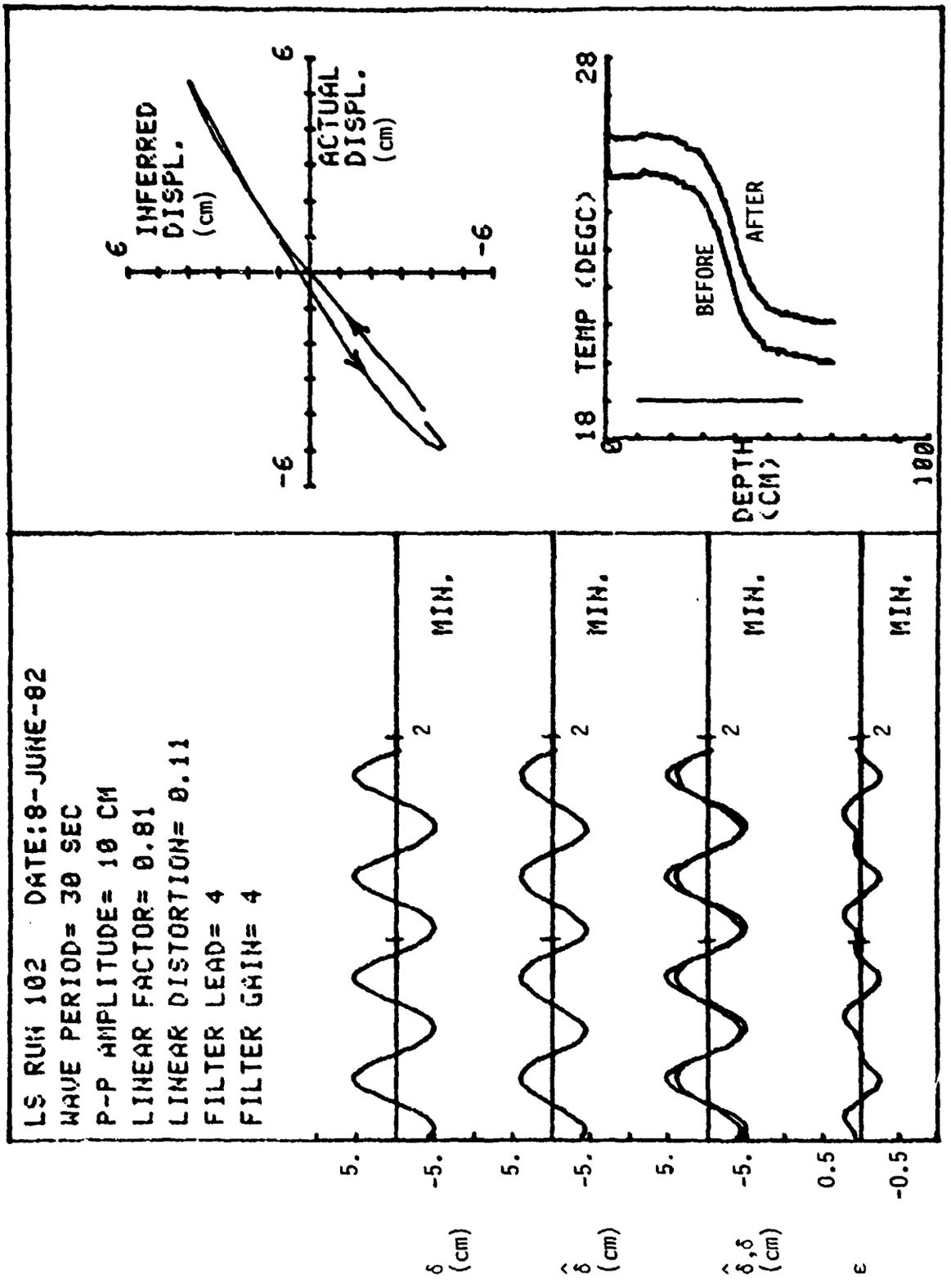

Figure 5.1.1 Results for Line Sensor Linearity Test; Stable Step Temperature Change

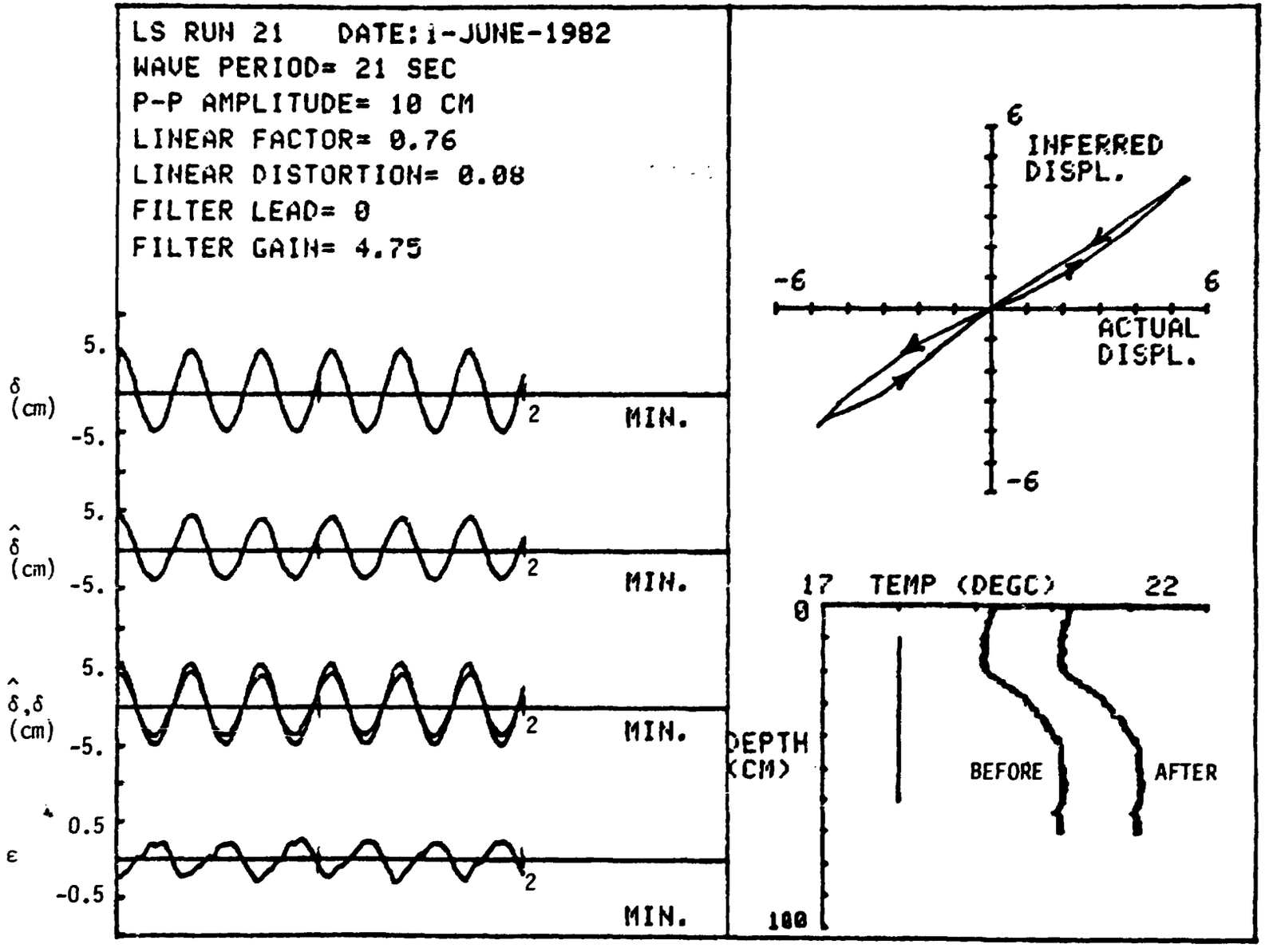

Figure 5.1.2 Results for Line Sensor Linearity Test; Unstable Temperature Profile (Fluid dynamic stability maintained with salt stratification.)

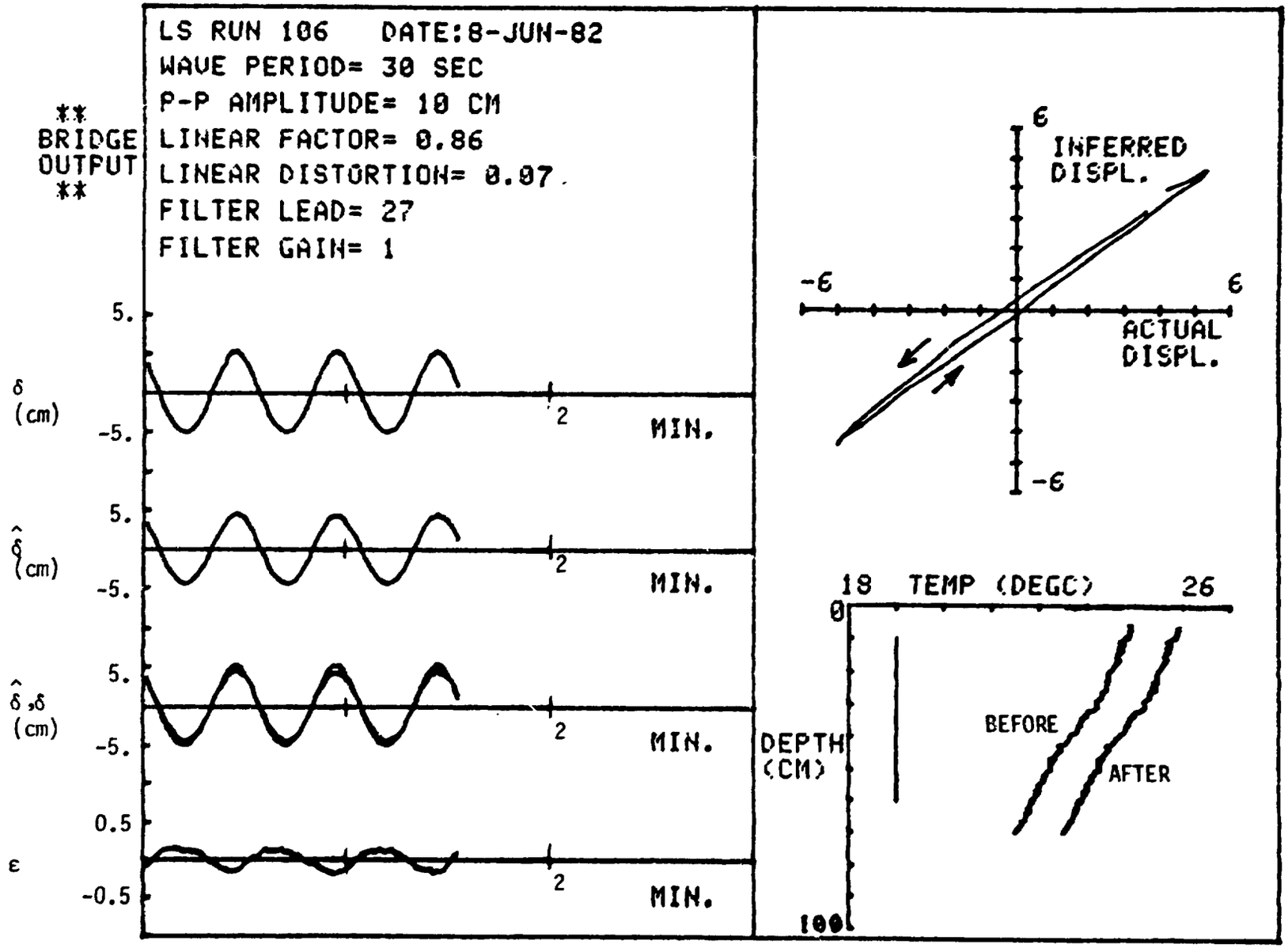

Figure 5.1.3 Results for Line Sensor Linearity Test; Linear Profile

$$|\varepsilon| < 0.14, \quad \text{and} \quad 0.86 < B < 1.14 \ .$$

Both the linear factor and instantaneous error (ε) were found to be in this range (or at least close,since measured values of B were in the range of 0.7 to 0.96 on most tests). However, it was a little disturbing that the linearity factor, B, was always found to be less than one. As yet, we have not found any reason for this, but it definitely appears that this parameter was inherently biased to the low side.

The inferred versus actual displacement plot would ideally be a 45° line bisecting the first and third quadrants. The line sensor approached this remarkably well. The linear distortion parameter, DD, is a measure of how much the actual plot of δ vs. $\hat{\delta}$ deviates from this 45° line. The distortion was found to always be less than 15% and, typically, was closer to 10%.

In summary, the line sensor response was found to be linear to within approximately 10%. The displacement at any given time could be calculated to within 24% using only the material properties of the Nickel wire and the measured electronic gain factors.

5.2 Response Time

This test was also performed in the stratified water tank. The line sensor probe was manually displaced as rapidly as possible and then held stationary. The unfiltered bridge voltage (V_b) was recorded on a digital oscilliscope. The line sensor's response in the form of $(V_b-(V_b)_\infty)/((V_b)_o-(V_b)_\infty)$ is shown on Figure 5.2.1 as the circled dots. The

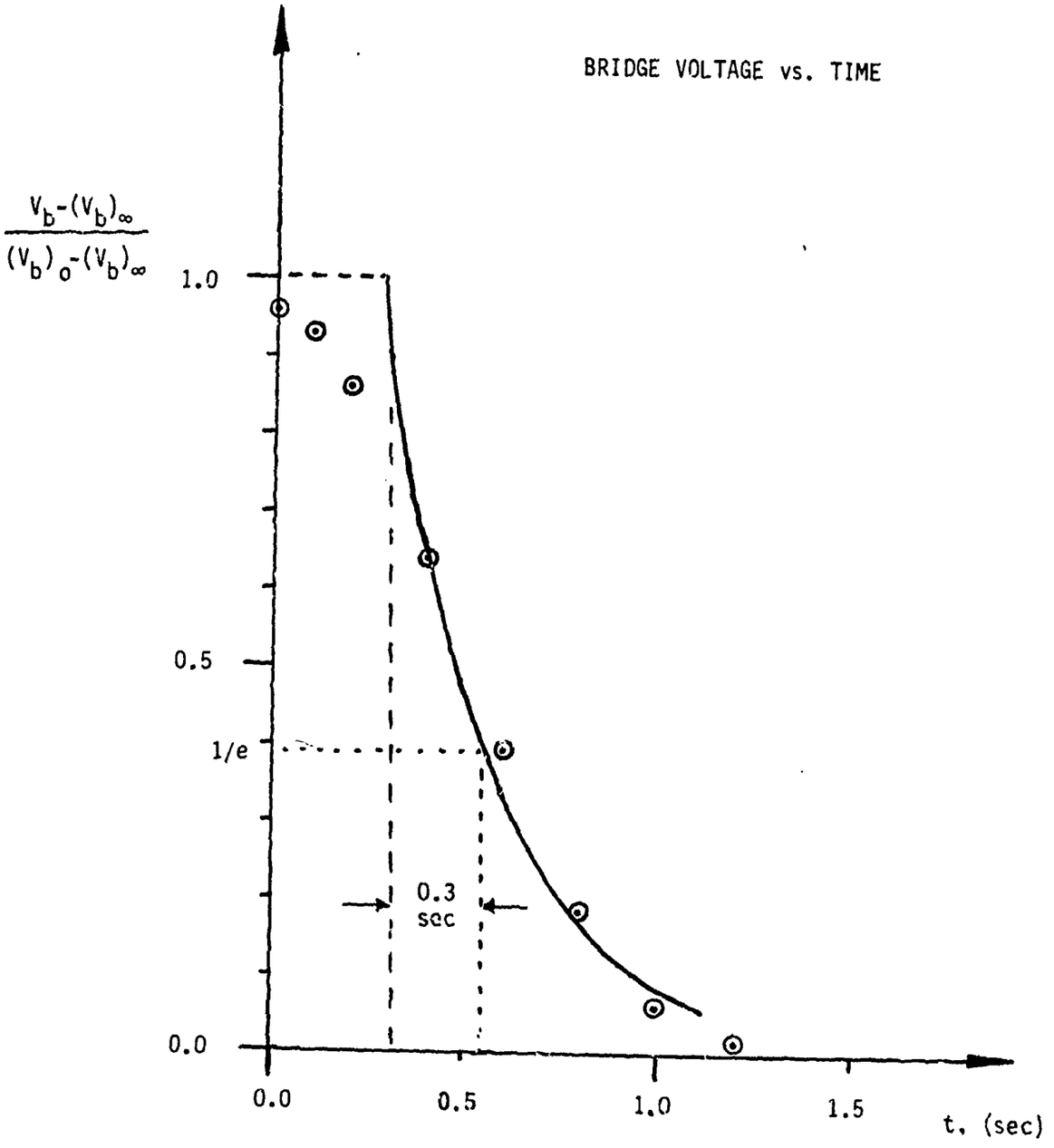

Figure 5.2.1 Line Sensor Response to a Sudden Displacement, ⊙

curve is the theoretical exponential recovery displaced to the right to account for the transient motion of the line sensor. The inferred time constant for the line sensor is on the order of 0.3 seconds. Clearly, this is more than adequate for studying oceanic internal waves with typical periods of 5 minutes and greater.

5.3 Effect of Thermal Finestructure

In theory,[3] the line sensor probe should be very insensitive to turbulence or finestructure whose vertical scale is smaller than the length of the probe. To test this characteristic, two experiments were performed. The first test consisted of generating a turbulent patch while running a linearity test (see Section 5.1). The patch was initiated approximately 20 seconds into the test by a vigorous stirring motion of a small paddle next to the line sensor. After 10 seconds of stirring, the patch spanned the width of the line sensor probe and was about 30 cm in height (just over half the probe height). Shadowgraphs obtained during the evolution and decay of the turbulent patch are illustrated in Figure 5.3.1.

The results of the linearity test conducted with a turbulent patch are presented in Figure 5.3.2. The initiation of the patch is indicated above the inferred displacement ($\hat{\delta}$) plot by the asterisk, and the vertical location of the patch relative to the line sensor is shown on the temperature profile (lower right corner). The linear factor (B) of 0.89 is a typical result for the linearity test, as are the linear distortion factor (DD = 0.13) and the instantaneous error ($|\varepsilon| < 0.25$). The turbulent patch clearly had, at most, only secondary effects on the linearity of the line sensor's response.

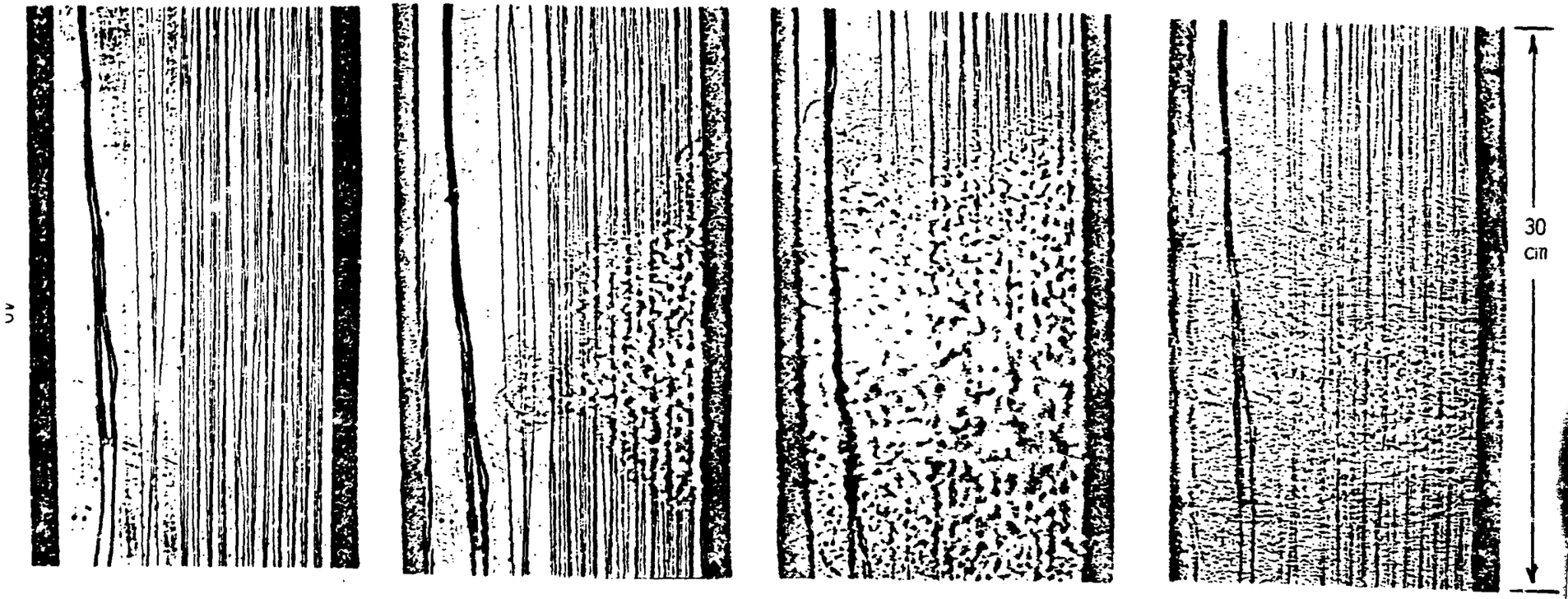

(a) Still Water (t = 0 sec)

(b) Patch Initiated (t = 20 sec)

(c) Fully Turbulent (t = 30 sec)

(d) Patch Decay (t = 90 sec)

Figure 5.3.1 Turbulent Patch Evolution and Decay

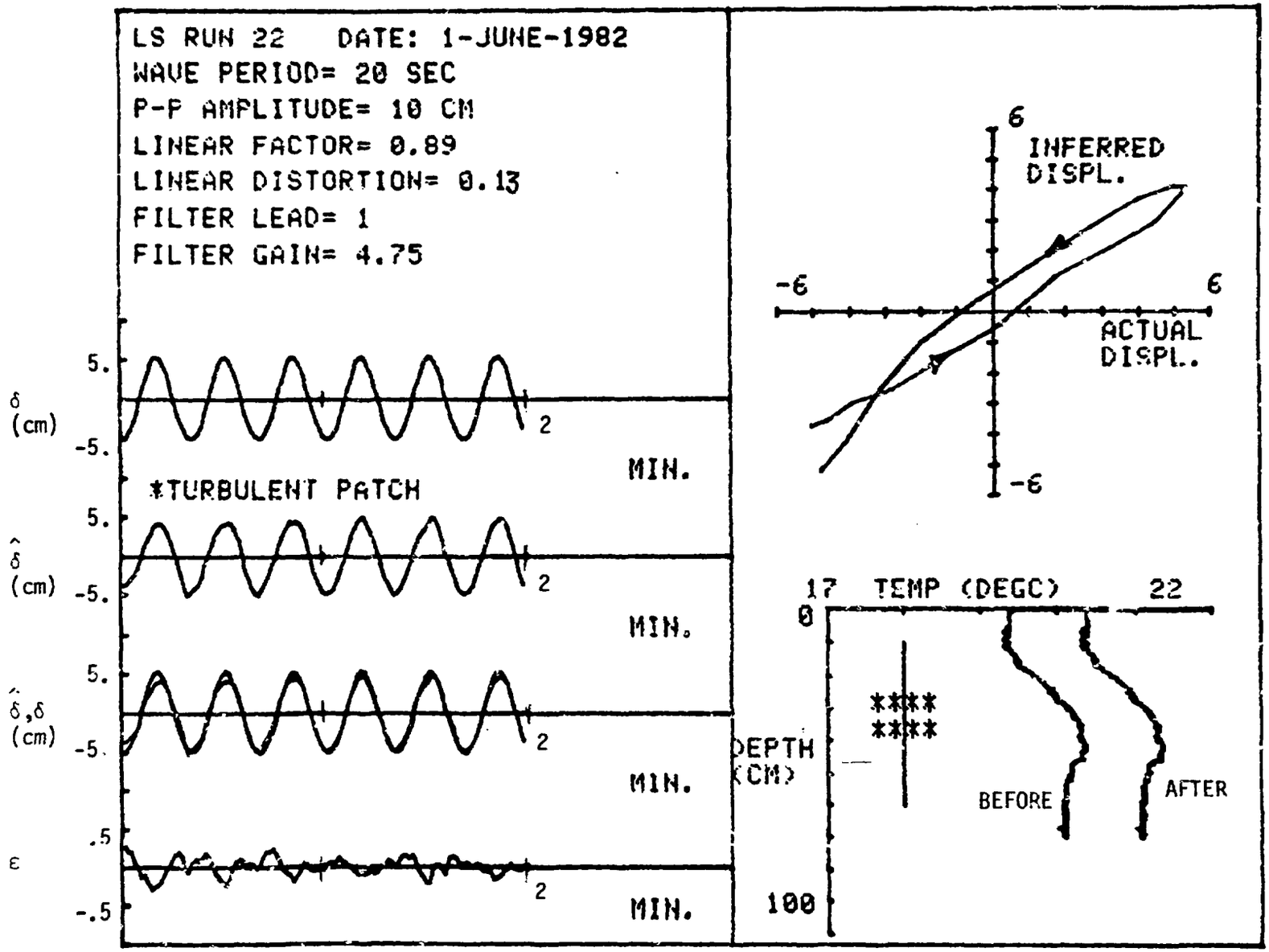

Figure 5.3.2 Results of Line Sensor Linearity Test With a Turbulent Patch Present

The second test was performed by generating internal waves in the stratified tank with the line sensor held stationary. It proved to be very difficult to generate a single wave mode as the wave generator drive motor had only rather coarse speed control. Hence, only occasionally were we able to generate a stable mode which would remain constant for the duration of a test (2 minutes).

With a reasonably steady wavefield in the tank, the filtered line sensor voltage (V_f) along with the voltage of a cold film probe (V_c) located at the approximate center of the line sensor were both recorded. After 1 minute's duration, a turbulent patch was generated by the method described above. The line sensor and cold film voltages for two such tests are plotted (in arbitrary units) in Figure 5.3.3 against time. Unfortunately, we were not able to generate the turbulent patch without affecting the internal wave (i.e., its amplitude increased, as can be seen in the figure). Nevertheless, the curves clearly illustrate the rapid and significant deterioration of a point sensor's (cold film probe) signal compared with the line sensor's signal.

5.4 Internal Waves - Effect of Strain

It is known that the (ideal) line sensor's response to displacements of an internal wave with strain present is not exactly linear.[3] Tests were performed to determine the linear distortion of the response of the prototype line sensor to an internal wavefield with strain. Internal waves were generated in the stratified water tank with the motor synchronized as close as possible to a natural tank mode. The waves generated had peak-to-peak displacement amplitudes on the order of 3 cm in the vertical (determined by dye

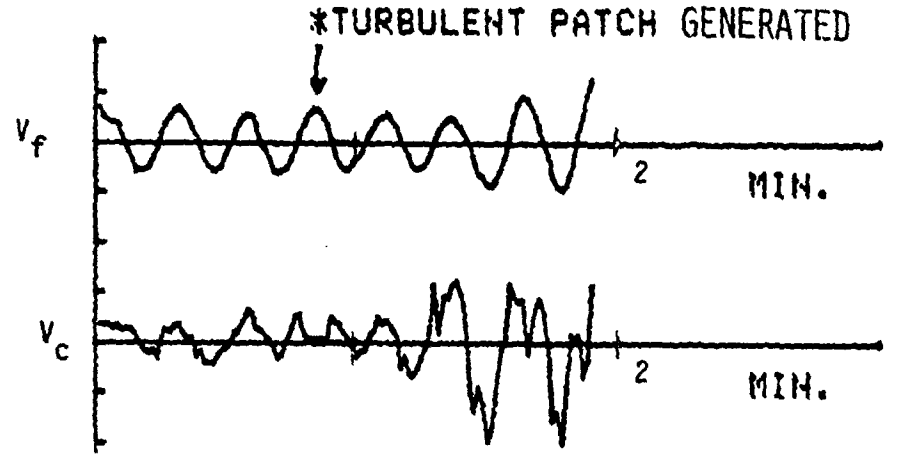

*TURBULENT PATCH GENERATED
V_f
2
MIN.
V_c
2
MIN.

Figure 5.3.3 The Filtered Line Sensor Voltage (V_f) and the Cold Film Probe Voltage (V_c) in the Presence of an Internal Wave With a Turbulent Patch Generated in 1 Minute.

streaks). Because of the modal structure of internal waves, the peak in the internal wave's displacement is located just below the center of the line sensor. At the top of the line sensor the vertical motions were negligible, and at the bottom it was on the order of 1 cm (peak-to-peak) in the vertical. Thus, the tank's internal waves had a vertical strain of about 4% (the 1 cm relative displacement over the approximately 25 cm semi-span of the line sensor) which is far greater than would ever be experienced in an oceanic situation. Although unimportant to the line sensor's response, the horizontal displacements caused by the internal waves were less than 2 cm at the center of the line sensor.

The variation of displacement of the wave over the vertical extent of the line sensor was extremely difficult to measure accurately. Additionally, it was not possible to accurately specify the actual wave displacement to be compared with the line sensor inferred displacement. To avoid these difficulties, comparison was made between the line sensor voltage (V_f) and the wave-maker displacement (potentiometer voltage, V_p). In order to sustain a steady wave for the test duration, it was necessary to carefully tune the wave-maker frequency to a natural wave frequency of the tank. Under these conditions the wave-maker and internal wave vertical displacements are directly proportional and, hence, the line sensor voltage and wave-maker displacement should be linearly related.

The instantaneous and average linear distortions were calculated respectively by:

$$\tilde{\varepsilon} \quad \frac{-KV_p}{|KV_p|_{max}} \quad , \text{ and}$$

$$\overline{DD} = \left[\frac{\sum (V_f - KV_p)^2}{\sum (KV_p)^2} \right]^{1/2} ,$$

where K is determined by a least squares fit:

$$V_f = KV_p \ .$$

The results of two internal wave tests are shown in Figures 5.4.1 and 5.4.2. The two signals V_f and KV_p are plotted in arbitrary units against time, individually and overlayed, just above the instantaneous distortion, $\tilde{\varepsilon}$. The average "linear distortion" is also given. The instantaneous distortion from a linear relation between the two displacements was typically less than 30% and the average linear distortion ranged from 10% to 25%.

It is appropriate here to remark again on the difficulty experienced in trying to obtain a single internal wave mode. Contamination of the dominant mode by other modes (both due to reflections from end walls and from the internal wave-maker itself) prevailed to some extent throughout all the internal wave tests. Thus, the distortion parameters calculated as differences between the wave-maker displacement (~ to the dominant internal wave displacement) and the line sensor response would be expected to be large due to this contamination of the wave mode. A conservative estimate of the contamination effect indicates that the average linear distortion of the prototype line sensor response would be from 5% to 20%. This represents a 5% increase over the linear distortion for strain free displacements (see linearity tests, Section 5.1).

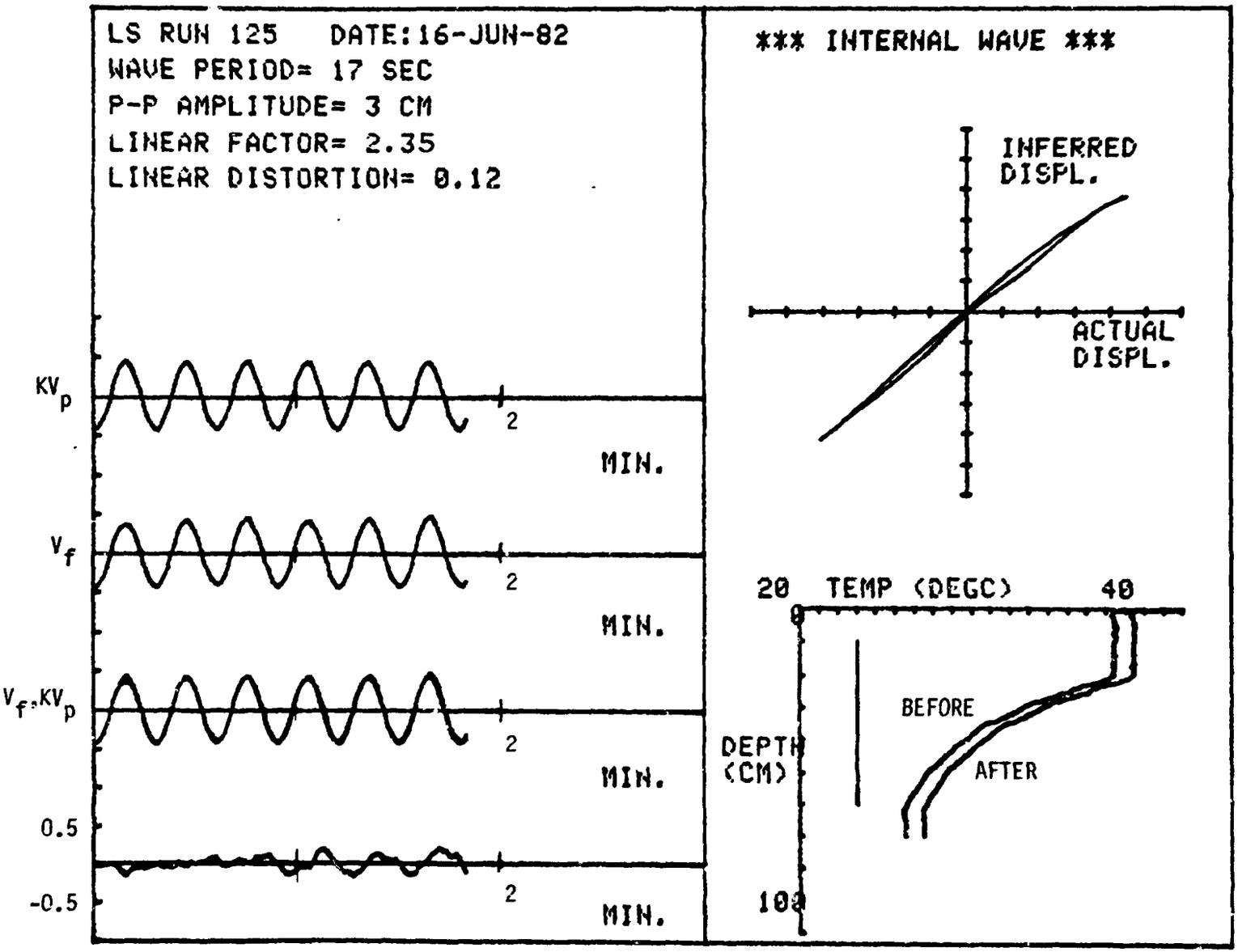

Figure 5.4.1 Results of an Internal Wave Test

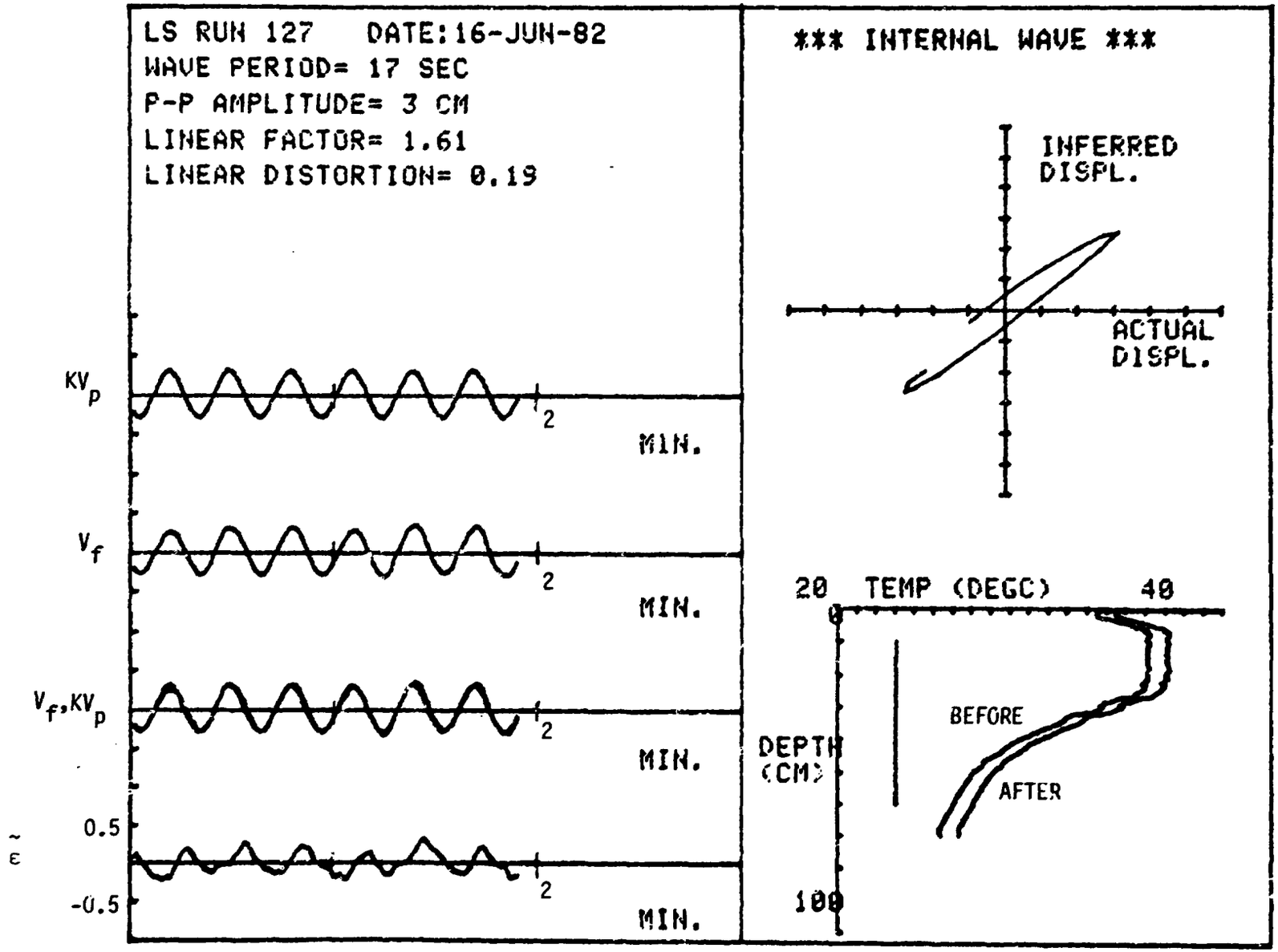

Figure 5.4.2 Results of an Internal Wave Test

5.5 Mechanical Considerations

An attractive feature of the prototype line sensor is its inherent ruggedness and durability. Following are four examples:

- Stability

The line sensor has been operated over a three month period without any apparent deterioration of its performance. During this period, it has remained suspended in salt water. The probe resistance has been checked periodically and remains unchanged within measurement accuracy (± 1%).

- Durability

During the three months of operation, the line sensor probe was handled extensively. It was inadvertently dropped on a concrete floor, stepped on, and bumped with hands, hammers and wrenches. In short, it has been handled fairly roughly and yet remains mechanically intact. The stainless steel frame and Teflon coated nickel wire have withstood three months of salt water immersion without signs of corrosion or deterioriation.

- Wire Insulation Loss

One concern with the line sensor design was the gradual rubbing away of the nickel wire insulation that might be experienced by an ocean probe during extended service. To check what effect this would have on the line sensor's response, a one inch strip of insulation was removed from the prototype sensor wire at approximately the center of its length to simulate this problem. At the time of writing of this report, the sensor has been suspended in salt water for 9 days with one inch of the wire bare and it still functions properly without any apparent signs of mechanical or performance deterioration.

- Protective Screens

As durable and rugged as the prototype proved to be, it was felt that an ocean going probe would probably require protective screen covers for the strung wire. There was some concern that the screens might alter the displacement field of a passing internal wave and thereby the sensor response. To test this, one-quarter inch mesh screens were installed on the prototype line sensor (Figure 5.5.1) for tests with internal waves. The line sensor output voltage traces (in arbitrary units) are shown in Figure 5.5.2. Unfortunately, due to time constraints, we were not able to obtain "good" internal waves (significant contamination by multiple mode interactions as described previously). Nonetheless, the traces clearly remain coherent and demonstrate that the protective screens have, at most, only a minor effect on the line sensor response.

5.6 Summary

The prototype line sensor has proven to be remarkably successful. Its response to a displacement field can be calibrated to within 15% with a maximum of 10% distortion for a strain free field. With unrealistically high strains, it can be calibrated to within 20% with a maximum of 15% distortion. The response time is extremely quick (~ 0.3 seconds), and the probe was found to be insensitive to microstructure contamination. Additionally, the line sensor has proven very rugged, durable, stable, and corrosion resistant.

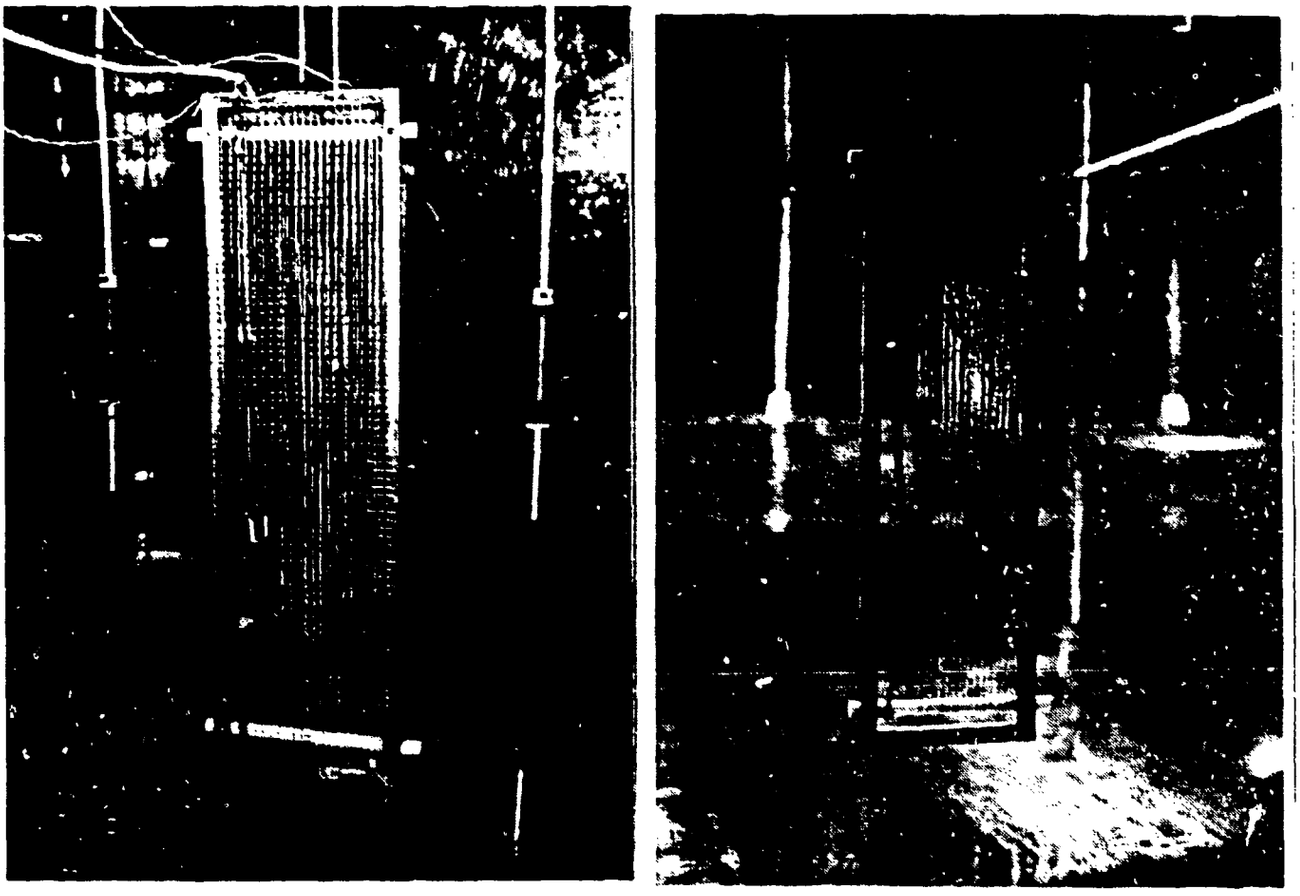

(a) (b)

Figure 5.5.1 Line Sensor Probe; (a) with 1/4 Inch Mesh Protective Screen, (b) Without Screen

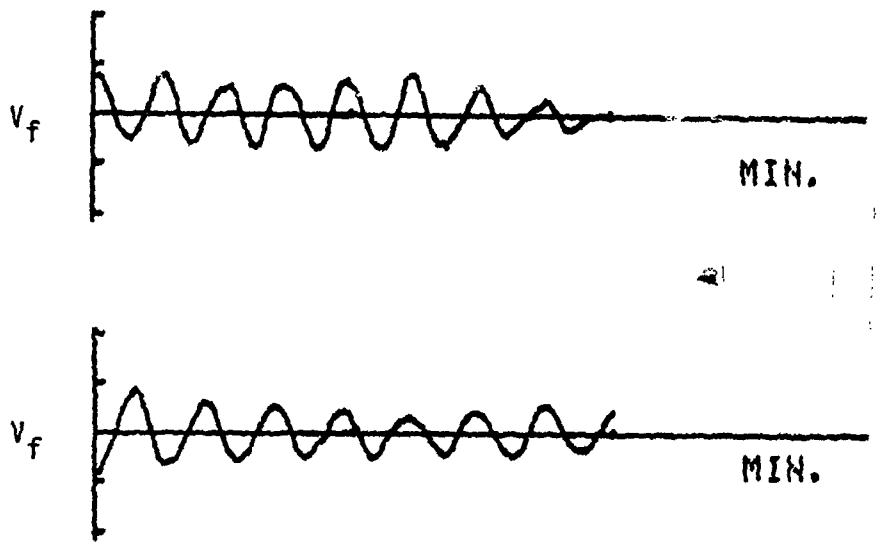

Figure 5.5.2 Two Line Sensor Output Voltage Traces With 1/4 Inch Mesh Screens Installed

6. RECOMMENDED OCEAN-GOING LINE SENSOR PROTOTYPE

The successful laboratory demonstration of the line sensor concept and the need within the Navy for a versatile, reliable internal wave monitoring instrument form a compelling motivation for further development of an ocean-going line sensor. The study by Dynamics Technology (DynaTech) has been designed to move directly to construction of a full-scale line sensor. As part of the present research, DynaTech has prepared a conceptual design of a recommended ocean-going line sensor prototype, including structural design (which follows directly from the laboratory prototype) and an integral circuit design.

6.1 Structural Design

As discussed in Section 3, the laboratory line sensor was designed as a subscale prototype of one module of an ocean-going version. In the analysis of the line sensor given in Section 2, it was determined that the sensor should be longer than the typical ocean finestructure vertical scale (~ 1 meter) to effectively "integrate out" any local temperature fluctuations present in the water which are displaced vertically by a passing internal wave field. Furthermore, to avoid significant second-order distortion of the line sensor signal caused by internal wave vertical strain, it was shown by Gran and Kubota[3] that the line sensor should be much shorter than the vertical wavelength of the internal wave.

Ideally, one would like to deploy a vertical array of line sensors as shown in Figure 6.1 and have the capability to monitor these line sensor "modules" individually or in various combinations (e.g., five 2-meter line

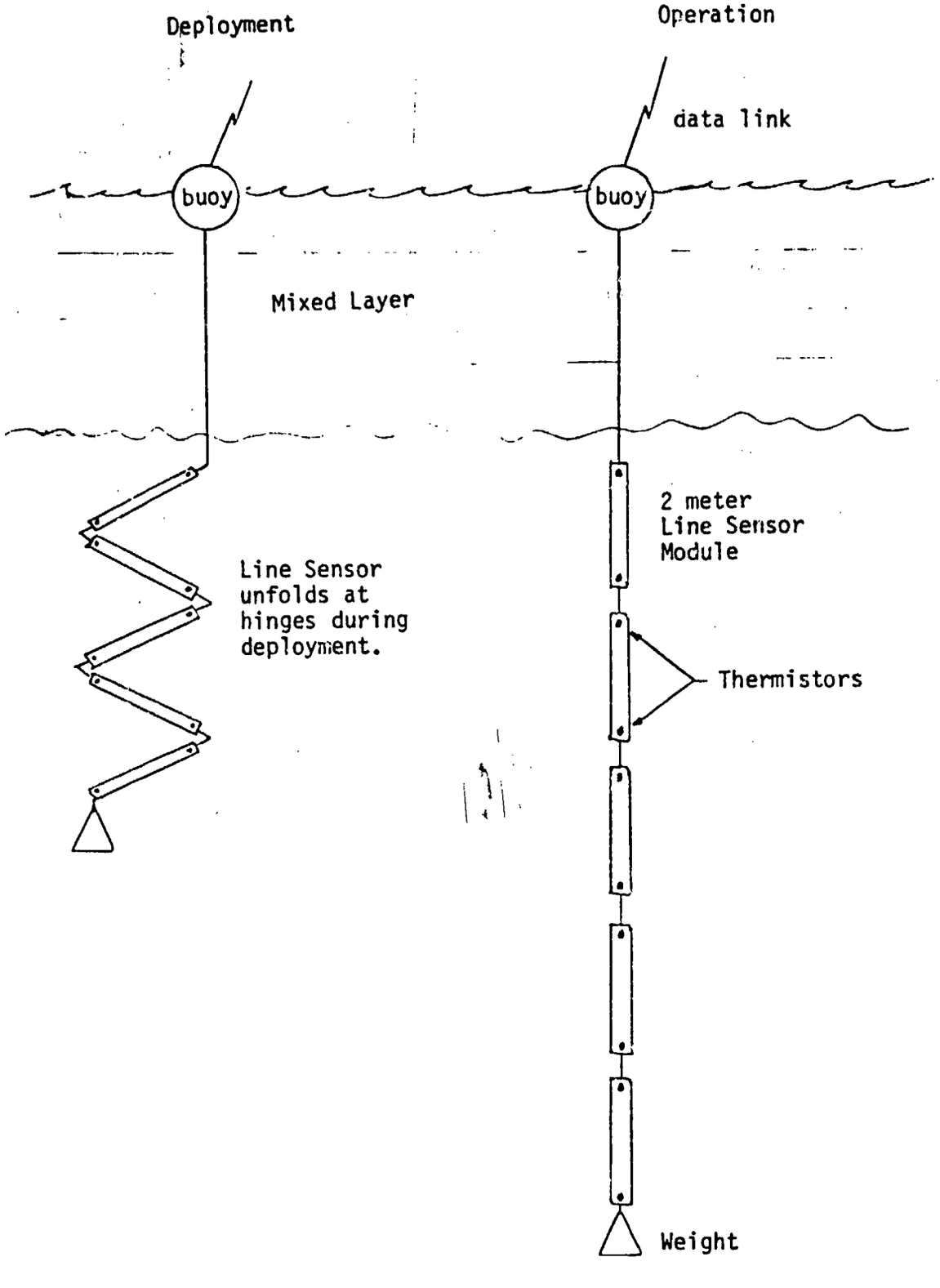

Figure 6.1. Sketch Of Ocean-Going Line Sensor Prototype and Deployment Scheme.

sensors, two 5-meter line sensors, etc.). This would allow one the additional capability of examining the modal structure of the internal wavefield, an important physical parameter in characterizing a local source which might generate relatively short (< 100 m) internal waves.

A practical constraint in designing a line sensor for field use is that it must be compact for storage and, perhaps, be ship-deployable and recoverable in fairly strong seas. Of course, it must also withstand normal deck handling operations. Another potentially desirable implementation would be to air drop several line sensors to achieve "area coverage" and internal wave propagational information.

With these guidelines in mind, we recommend that a prototype ocean-going line sensor be constructed consisting of, for example, five to ten line sensor modules each 1 meter long and hinged together as shown in the sketch in Figures 6.1 and 6.2. This hinged design would allow the line sensor to be compactly stored aboard ship, or within a protective "box" for aerial deployment. Each module would be an extended version of the prototype line sensor successfully tested in the laboratory. In addition, each module will be strung with several line sensor loops to provide redundancy in case of an isolated failure.

Recall from equation (2.11) that the local ocean temperature gradient is required to infer the fluid displacement. This can be obtained most easily by mounting thermistors at the top and bottom of each line sensor module, as indicated in Figure 6.2. The thermistor data from sequential modules can then be used to calculate the mean temperature profile.

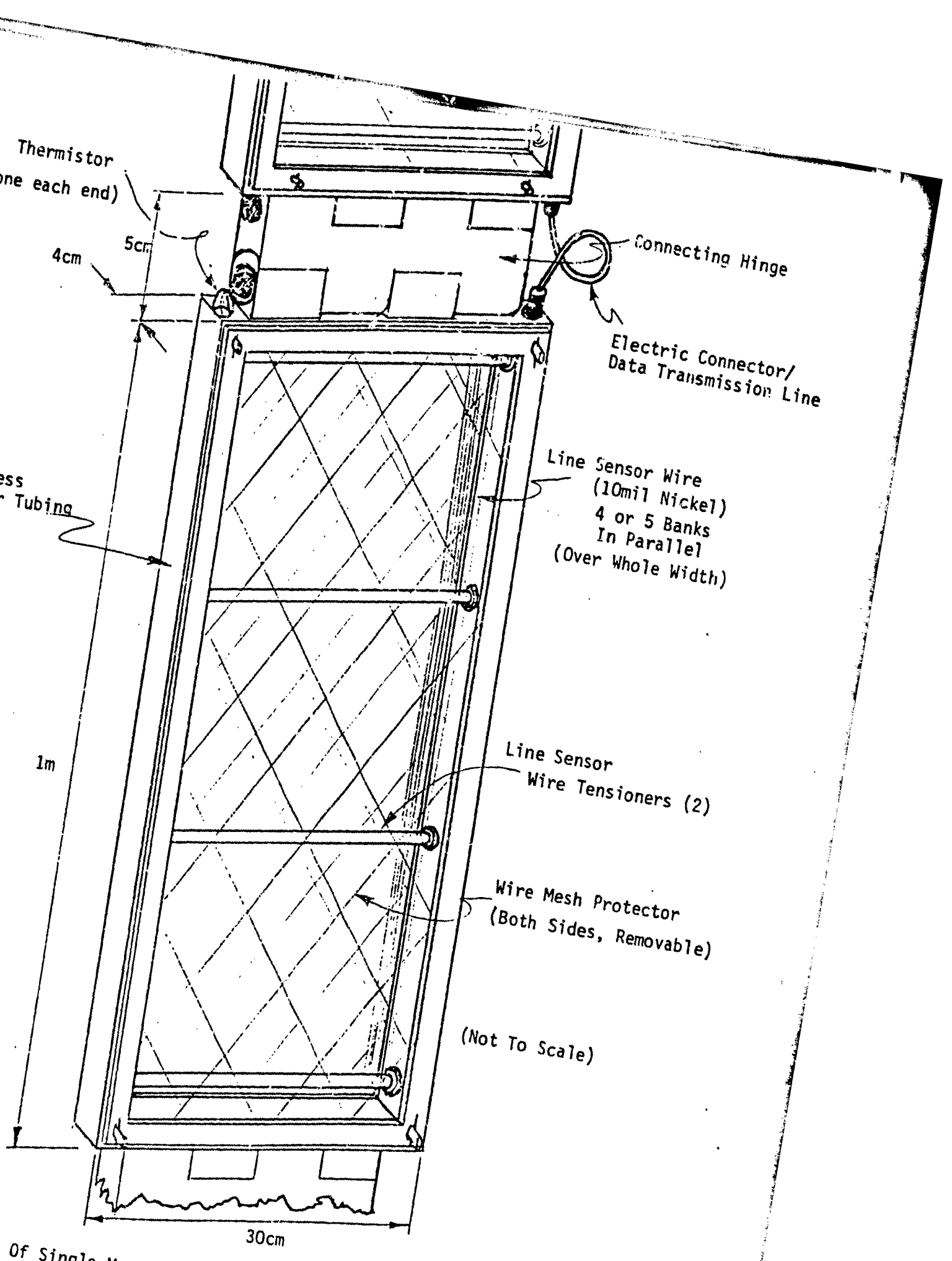

Figure 6.2. Sketch Of Single Module And Hinge Detail For Ocean-Going Line Sensor.

6.2 Electronic Design

The proposed line sensor circuit layout will support several modules, each containing a few separate line sensor elements and two thermistors. Each module will house one analog signal conditioning circuit for each transducer plus one data conversion unit (digital section) per module. Digitized data from each module will be sent along a serial transmission line (bussed to all modules) to a minicomputer (or dedicated chip) which can preprocess the data, if necessary, and record or transmit that data elsewhere. Each module will be connected to a common ±15V and +5V power supply line or battery. Although physically connecting two or more adjacent line sensors on a module together and treating the combination as a single transducer would reduce the amount of data collected, there is no advantage in adding this flexibility since, at the low data rates under consideration, there will be adequate time for the minicomputer to average signals from adjacent sensors.

Analog Signal Conditioning

Bridge supply: In the interest of assuring a stable supply voltage, the transducer bridges are excited by +10V reference source instead of the +15V power supply. The advantage in doing this is that the bridge excitation can be made insensitive to variations in power supply voltage. An Analog Device AD2700 voltage reference gives .006% drift over a 20°C temperature change. This IC and the others in the analog section should be capacitively decoupled from the ±15V supply.

Line Sensor: This section is very similar to the laboratory circuit (see Figure 6.3). Since the stable voltage is +10V instead of +15V, the dropping resistor above the bridge has been reduced to 1KΩ to maintain the same excitation at the top of the bridge. The 100μf capacitor connected to the top of the bridge minimizes any surges from the reference voltage, and the reference voltage will be buffered through a voltage follower.

The line sensor is shown in the lower right leg of the bridge while the lower left leg serves as a balancing leg. The bridge output is amplified by 10,000 and a capacitor is added to act as a low pass filter. The MP5507 has been used successfully in the lab for this amplifier.

Thermistors: The thermistor shown in Figure 6.4 has been placed in the bottom half of a voltage divider. The bridge output is amplified and low pass filtered (16 Hz) in the first stage, then high pass filtered at 0.15 Hz. The signal is then buffered and again filtered (low pass) at 16 Hz.

Data Conversion/Digital Circuitry: Since all analog signals from each module will eventually be converted to digital signals through one A/D converter, they must be multiplexed onto the input of the A/D subsystem. The circuitry which accomplishes this is shown in Figure 6.5. Since control, data acquisition and transmission are all done slowly, there are only three requirements for the microcomputer. First, for simplicity, it should be a single component computer. Second, there must be enough I/O lines available (22 bits in the design under consideration), and finally it should contain an EPROM. Intel's 8748 and Mostek's MK38P70/02, and MK38CP70/02 satisfy these requirements.

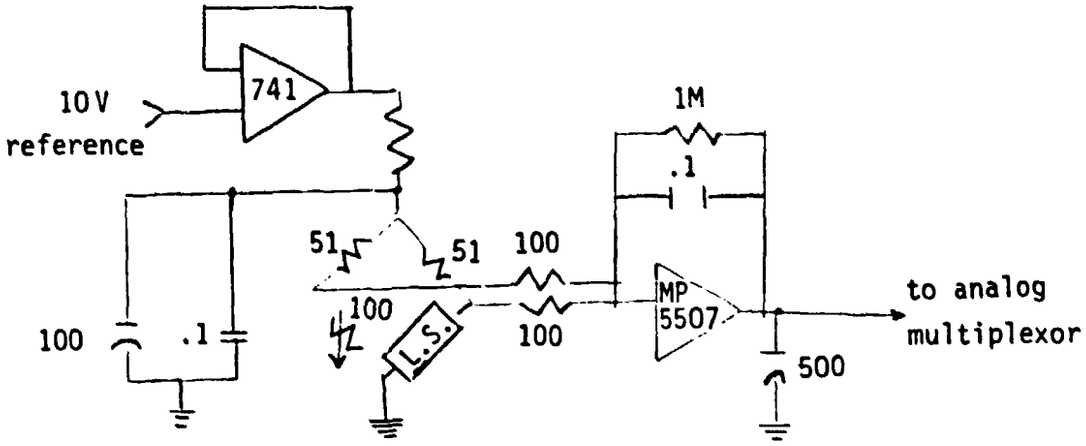

Figure 6.3. Line Sensor Circuit Schematic

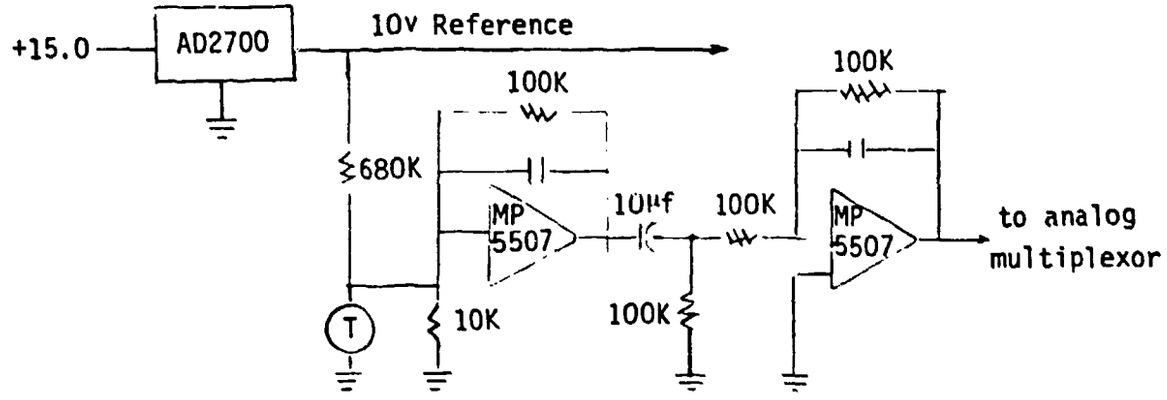

Figure 6.4. Thermistor Circuit Schematic.

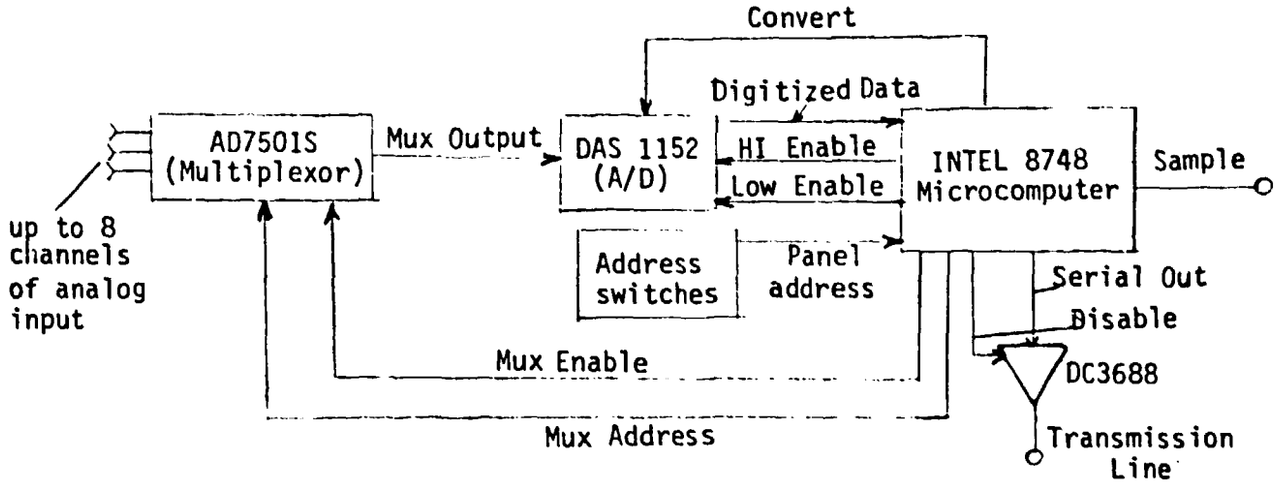

Figure 6.5. Data Conversion/Digital Section (one per line sensor module)

To minimize the number of cables running down to the sensors, data from the microcomputer on each of the modules will be sent up a common transmission line. A program must be written in order for the microcomputer to control data acquisition. The most convenient way of doing this is with a microcomputer "development system" (a programming system). Such a system consists of a minicomputer built around the microcomputers being used in the line sensor modules. (This whole process "hardwires" in the line sensor signal processing.) Since the program stored in an EPROM is (almost) permanent, the operator can simply turn on the line sensor and the microcomputer will execute its routine. Changes can be made fairly easily by erasing the EPROM and reprogramming it.

The microcomputer output from each module is readily multiplexed to a recorder or data transmitter.

7. SUMMARY AND CONCLUSIONS

Under the sponsorship of the DESAT program, Dynamics Technology, Inc. has designed, constructed and successfully tested a laboratory prototype of a line temperature sensor, or "line sensor," which may be used for measuring internal wave-induced fluid displacements in the ocean. This sensor has distinct advantages over presently used internal wave measurement techniques such as thermistor chains and "yo-yo" profilers, which require both enormous amounts of data and sophisticated processing to try to remove finestructure contamination in order to resolve the shorter wavelength internal waves often associated with a localized source. Properly designed, the line sensor output is virtually linearly proportional to the internal wave fluid displacement, and it is easily calibrated.

An analysis of the basic line sensor operating principle was given in Section 2 which identified the expected response of the sensor and design constraints for an ocean-going version. Laboratory experiments on the prototype sensor, designed to simulate an ocean sensor as closely as possible, have shown that the analytically inferred fluid displacement was within 20% of the true displacement and the predicted linearity was within 10% (i.e., correct to within experimental accuracy). Furthermore, the line sensor was shown to be unaffected by turbulent patches (similar to ocean finestructure) which is one of the main advantages of the line sensor over more conventional internal wave monitoring techniques.

A conceptual design for an ocean-going line sensor which could be built in the next phase of the line sensor's development program was presented in Section 6. It is essentially a scaled up version of the successful laboratory

prototype, and employs several line sensor modules hung in series. Practical constraints such as deployment in moderate seas and deck handling have been factored into the conceptual design. Revised and improved circuitry has also been identified which permits flexible multiple combination line sensor signal processing (in situ digitization on each line sensor module with data being multiplexed and recorded by a single minicomputer mounted in a near-surface buoy, for example) and which draws upon our experience from the laboratory prototype tests.

In conclusion, we find that the line sensor concept has been successfully demonstrated in the laboratory. We recommend that a full-scale prototype development be initiated to validate the performance of such an internal wave measurement system in an oceanic setting.

REFERENCES

1. Konvayev, K.V. and Sabinin, K.D. (1972) "New Data on Internal Waves in the Ocean Obtained With Distributed Temperature Sensors," Doklady Akad. Nauk SSSR, 209 (Geophysics).

2. Brekhovskikih, L.M., Konjaev, K.V., Sabinin, K.D. and Serikov, A.N. (1975) "Short-Period Internal Waves in the Sea," J. Geo. Res., 80, No. 6, February.

3. Gran, R.L. and Kubota, T. (1977) "The Response of a Distributed Linear Temperature Sensor to Internal Waves in a Microstructure-Laden Ocean," Dynamics Technology Report DT-7601-21.

4. Neshyba, S. and Denner, W.W. and Neal, V.T. (1972) "Spectra of Internal Waves: In-Situ Measurements in a Multiple-Layered Structure," J. Phys. Ocean., V. 2, p. 91, January.